doi:10.1016/j.jmb.2011.03.054 J. Mol. Biol. (2011) 410, 896–916

Contents lists available at www.sciencedirect.com

Journal of Molecular Biology

journal homepage: http://ees.elsevier.com.jmb

T-Cell Receptor Signaling Enhances Transcriptional Elongation from Latent HIV Proviruses by Activating P-TEFb through an ERK-Dependent Pathway

Young Kyeung Kim, Uri Mbonye, Joseph Hokello and Jonathan Karn*

Department of Molecular Biology and Microbiology, School of Medicine, Case Western Reserve University, 10900 Euclid Avenue, Room W200, Cleveland, OH 44106-4960, USA

Received 4 February 2011; received in revised form 20 March 2011; accepted 24 March 2011

Edited by M. F. Summers

Keywords:
HIV latency;
HIV transcription;
P-TEFb;
T-cell receptor signaling;
ERK signaling

Latent human immunodeficiency virus (HIV) proviruses are thought to be primarily reactivated *in vivo* through stimulation of the T-cell receptor (TCR). Activation of the TCR induces multiple signal transduction pathways, leading to the ordered nuclear migration of the HIV transcription initiation factors NF-κB (nuclear factor κB) and NFAT (*n*uclear *f*actor of *a*ctivated *T*-cells), as well as potential effects on HIV transcriptional elongation. We have monitored the kinetics of proviral reactivation using chromatin immunoprecipitation assays to measure changes in the distribution of RNA polymerase II in the HIV provirus. Surprisingly, in contrast to TNF-α (tumor necrosis factor α) activation, where early transcription elongation is highly restricted due to rate-limiting concentrations of Tat, efficient and sustained HIV elongation and positive transcription elongation factor b (P-TEFb) recruitment are detected immediately after the activation of latent proviruses through the TCR. Inhibition of NFAT activation by cyclosporine had no effect on either HIV transcription initiation or elongation. However, examination of P-TEFb complexes by gel-filtration chromatography showed that TCR signaling led to the rapid dissociation of the large inactive P-TEFb:7SK RNP (small nuclear RNA 7SK ribonucleoprotein) complex and the release of active low-molecular-weight P-TEFb complexes. Both P-TEFb recruitment to the HIV long terminal repeat and enhanced HIV processivity were blocked by the ERK (extracellular-signal-regulated kinase) inhibitor U0126, but not by AKT (serine/threonine protein kinase Akt) and PI3K (phosphatidylinositol 3-kinase) inhibitors. In contrast to treatment with HMBA (hexamethylene bisacetamide) and DRB (5,6-dichlorobenzimidazole 1-β-ribofuranoside), which disrupt the large 7SK RNP complex but do not stimulate early HIV elongation, TCR

*Corresponding author. E-mail address: jonathan.karn@case.edu.

Present address: Y. K. Kim, Division of Molecular and Life Sciences, Pohang University of Science and Technology, Pohang, Korea.

Abbreviations used: HIV, human immunodeficiency virus; TCR, T-cell receptor; P-TEFb, positive transcription elongation factor b; RNAP, RNA polymerase; TAR, transactivation response region; CycT1, cyclin T1; CDK, cyclin-dependent kinase; NELF, negative elongation factor; DRB, 5,6-dichlorobenzimidazole 1-β-ribofuranoside; NF-κB, nuclear factor κB; TNF-α, tumor necrosis factor α; LTR, long terminal repeat; ERK, extracellular-signal-regulated kinase; mAb, monoclonal antibody; CsA, cyclosporin A; ChIP, chromatin immunoprecipitation; MAPKK, mitogen-activated protein kinase kinase; PI3K, phosphatidylinositol 3-kinase; PHA, phytohemagglutinin; TSA, trichostatin A; HMBA, hexamethylene bisacetamide; PMA, phorbol 12-myristate 13-acetate; Bistris, 2-[bis(2-hydroxyethyl)amino]-2-(hydroxymethyl)propane-1,3-diol.

signaling provides the first example of a physiological pathway that can shift the balance between the inactive P-TEFb pool and the active P-TEFb pool and thereby stimulate proviral reactivation.

Introduction

Human immunodeficiency virus (HIV) is able to evade antiviral immune responses and antiretroviral therapy by establishing latent infections, most notably in the long-lived resting memory $CD4^+$ T-cell population (for reviews, see Pierson *et al.*,[1] Coiras *et al.*,[2] and Alexaki *et al.*[3]). These latent infections are the major obstacle to virus clearance, and the virus will rapidly rebound from the latent reservoir following the interruption of antiretroviral therapy even in patients undergoing highly active antiretroviral treatment, where plasma viremia has been undetectable for many years.[4–6] Unfortunately, intensification of antiretroviral therapy does not appreciably deplete the residual viremia of patients on therapy.[7] The failure of current therapy to eradicate HIV has prompted renewed efforts to define the molecular mechanisms leading to HIV latency and to develop new therapeutic tools to attack latently infected cells.[8–10]

HIV transcription is dependent on the expression of the viral transactivator protein Tat, which fuels a powerful feedback mechanism (for reviews, see Peterlin and Price,[11] Karn,[12] and Singh and Weinberger[13]). In the absence of Tat, transcription initiation is normal, but elongation is highly restricted, and only short abortive transcripts are produced. Tat acts to stimulate transcription elongation by recruiting the cellular transcriptional elongation factor positive transcription elongation factor b (P-TEFb)[14] to nascent RNA polymerases (RNAPs) that have transcribed through the HIV transactivation response region (TAR) element, an RNA stem–loop structure found at the 5′ end of all viral transcripts. The form of P-TEFb used to stimulate HIV transcription is a complex of human cyclin T1 (CycT1), which is an RNA-binding protein that cooperatively binds to TAR RNA together with Tat and cyclin-dependent kinase (CDK) 9, a protein kinase that phosphorylates a variety of proteins within the elongating transcription complex. These phosphorylation events result in both the removal of the block to elongation through the targeting of the E (RD) subunit of the negative elongation factor (NELF)[15] and positive events that include the phosphorylation of the C-terminal domain of RNAP II[16] and Spt5 (*supp*ressor of *Ty 5* homolog), a subunit of the 5,6-dichlorobenzimidazole 1-β-ribofuranoside (DRB) sensitivity-inducing factor that enhances transcriptional elongation.[17,18]

Because Tat functions as part of a positive regulatory circuit, conditions that restrict transcription initiation will in turn cause a reduction in Tat levels to below threshold levels and lead to the establishment of latency.[19,20] Typically, epigenetic silencing of HIV transcription initiation provides the trigger that drives viruses into latency. Key silencing events include the establishment of heterochromatic structures through the recruitment of histone deacetylases,[21–23] induction of histone methylation,[24–27] and DNA methylation.[28,29] In addition, there have been documented examples of HIV silencing through promoter occlusion when the viruses have integrated into actively transcribed genes.[30–32] However, even in these instances, establishment of heterochromatic structures on the latent provirus appears to contribute to the silencing of HIV transcription. These epigenetic blocks can be effectively reversed by the transcriptional initiation factors nuclear factor κB (NF-κB) and NFAT (*n*uclear *f*actor of *a*ctivated *T*-cells).[24,25,33,34] Both quiescent T-cells and Jurkat T-cells restrict HIV transcription initiation by sequestering the cellular transcription initiation factors NF-κB and NFAT in the cytoplasm.[35,36]

In actively replicating cells such as HeLa cells and Jurkat T-cells, P-TEFb activity is tightly regulated, and the majority of the enzyme is sequestered into a large inactive 7SK RNP (small nuclear RNA 7SK ribonucleoprotein complex) comprising 7SK RNA and a series of RNA-binding proteins.[37,38] Essential components of the 7SK RNP complex include the following: HEXIM (hexamethylene bis-acetamide inducible gene) 1 or HEXIM2, which inhibits CDK9 kinase in a 7SK-dependent manner;[39,40] LARP-7 (*La r*ibonucleo*p*rotein domain family, member *7*), a La-related protein bound to the 3′ UUU-OH sequence of 7SK;[41,42] and BCDIN3 (methyltransferase BCDIN3D), a methylphosphate-capping enzyme specific for 7SK.[43] The sequestration of enzymatically active P-TEFb in the cell provides an additional block to efficient transcription elongation from the HIV promoter. Tat overcomes this barrier by disrupting the 7SK RNP complex by competitively displacing HEXIM1.[44–46]

Resting $CD4^+$ T-cells further ensure that latent proviruses remain transcriptionally inactive by restricting both the level of CycT1[47] and the level of phosphorylated CDK9, which is the enzymatically active form of the enzyme.[47,48] Similarly, in unstimulated monocytes, translation of CycT1 is blocked by miR-198.[49]

Recently, we have developed model systems for studying HIV latency using lentiviral vectors that express attenuated Tat genes in cis.[24,25] Detailed kinetic studies have emphasized that proviral

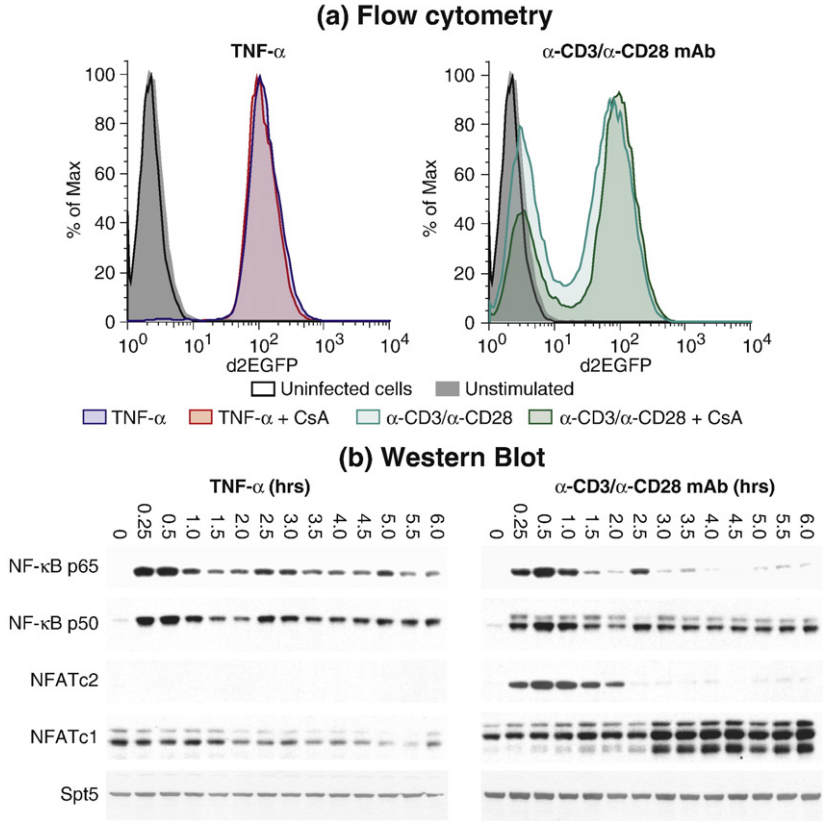

Fig. 1. Induction of latently infected 2D10 cells by stimulation of the TCR. (a) Analysis of HIV proviral activation by flow cytometry. Cells were activated with 10 ng/ml TNF-α (left) or α-CD3 mAb plus α-CD28 mAb (right) in the presence or in the absence of CsA. Note that CsA did not prevent proviral reactivation following TCR signaling. (b) Nuclear protein levels of the NF-κB subunits p65 and p50 and the NFAT family members NFATc1 and NFAFc2 were monitored during a 6-h time course. Western blot analysis of nuclear proteins following stimulation of 2D10 cells with 10 ng/ml TNF-α (left) or 0.125 μg/ml α-CD3 mAb plus 1 μg/ml α-CD28 mAb (right).

reactivation following NF-κB mobilization by tumor necrosis factor α (TNF-α) results in sequential waves of RNAP II recruitment to the long terminal repeat (LTR) as NF-κB enters and exits the nucleus, but virtually no downstream RNAP II until Tat is synthesized 2–4 h after stimulation.[25,33,50] In order to define the mechanisms of proviral activation following T-cell receptor (TCR) activation, we performed a similar kinetic analysis of proviral induction. We found unexpectedly that TCR signaling results in the immediate activation of transcription elongation, even at times when Tat levels are too low to sustain transcription elongation. This early increase in elongation is due to the activation of P-TEFb by the disruption of the 7SK RNP complex through the extracellular-signal-regulated kinase (ERK) pathway.

Results

Induction of latent provirus by TCR activation

The 2D10 cell line is a latently infected Jurkat T-cell line that carries a lentiviral vector expressing the regulatory proteins Tat and Rev in cis and a short-lived green fluorescent protein, d2EGFP (destabilized enhanced green fluorescent protein), in place of Nef.[25] The provirus in 2D10 cells also carries the H13L mutation in Tat, which effectively supports HIV transcription elongation but is attenuated and therefore helps to promote proviral entry into latency.[24,25,51] Extensive characterization of the 2D10 cell line has shown that the provirus is inserted into the first exon of the SEPX1 (*se*lenop*r*otein *X*, *1*) gene in opposite orientation to the SEPX1 promoter.[25]

An important advantage of 2D10 cells is that although HIV gene expression is highly suppressed (more than 98% of uninduced cells are d2EGFP negative), the cells are readily induced. For example, over 99% of the cell population becomes d2EGFP positive (mean fluorescent intensity >20) after exposure to 10 ng/ml TNF-α for 18 h (Fig. 1a). The provirus in 2D10 cells can also be efficiently reactivated by stimulation of the TCR using a combination of α-CD3 monoclonal antibody (mAb) and α-CD28 mAb. As shown in Fig. 1a, mAb stimulation of the TCR resulted in 62.4% reactivation of the latent proviruses (Fig. 1a).

In addition to activating NF-κB, TCR stimulation induces a complex cascade of pathways, including activation of NFAT through the Ca^{2+}–calcineurin pathway. This raises the intriguing possibility that HIV proviral reactivation following TCR stimulation involves multiple transcription factors in addition to NF-κB. In order to monitor the kinetics of activation of transcription factors following TCR

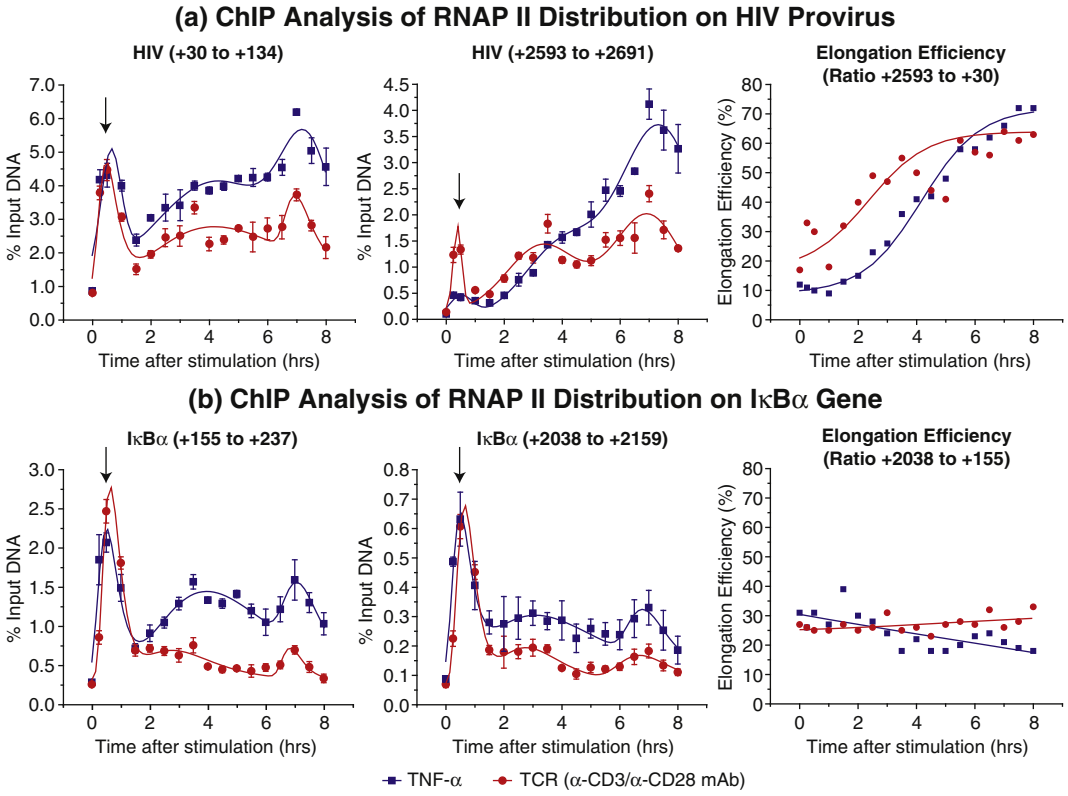

Fig. 2. Stimulation of HIV transcriptional elongation following TNF-α stimulation and TCR-mediated activation of latent proviruses. ChIP assays performed using RNAP II antibodies (N-20; Santa Cruz Biotechnology) were used to measure RNAP II distributions in the HIV provirus and the IκBα gene in clone 2D10 cells. (a) HIV transcription. Left: RNAP II levels at the transcription start site (HIV, +30 to +134). Throughout this figure, ChIP data sets were fitted to a series of overlapping Gaussian distributions as described in Materials and Methods. Middle: RNAP II levels at a downstream region (HIV, +2593 to +2691). Right: HIV elongation efficiency as measured by the ratios of RNAP II at +2593 and +30. The data were fitted to a biphasic curve. (b) IκBα gene elongation efficiency as measured by the ratios of RNAP II levels at +2038 and +155. Left: RNAP II levels near the transcription start site (IκBα, +155 to +237). Middle: RNAP II levels at a downstream region (IκBα, +2038 to +2159). Right: IκBα elongation efficiency as measured by the ratios of RNAP II at +2038 and +155. The data were fitted to a straight line. Blue lines and squares: activation of 2D10 cells with 10 ng/ml TNF-α. Red lines and circles: activation of 2D10 cells with 0.125 μg/ml α-CD3 mAb plus 1 μg/ml α-CD28 mAb. Note that activation through the TCR results in more than twice the amount of RNAP II reaching the downstream regions of the HIV provirus than is seen following activation by TNF-α.

stimulation, we compared the nuclear levels of NF-κB (p65 and p50) and NFAT (NFATc1 and NFATc2) following either TNF-α treatment or stimulation of the TCR with α-CD3/α-CD28 mAb by Western blot analysis (Fig. 1b). During a 6-h time course, TNF-α induced the cycling of the NF-κB p65 and p50 subunits between the cytoplasm and the nucleus.[25,33,50] After an initial peak of nuclear accumulation at 30 min, both NF-κB p65 and p50 levels oscillated at a period of approximately 2.5 h. As expected, there was no detectable increase in the nuclear levels of either NFATc1 or NFATc2 following TNF-α treatment. NFATc2 was undetectable in the nucleus prior to TNF-α exposure, whereas NFATc1 showed moderate nuclear levels in unstimulated cells, which slowly fell during the 8-h time course.

Stimulation of the TCR with α-CD3/α-CD28 mAbs activated both NF-κB and NFAT with unique kinetics (Fig. 1b). Initially, entry of NF-κB p65 into the nucleus followed kinetics that were nearly identical with those observed following TNF-α stimulation, and nuclear p65 levels reached a maximum at 30 min. However, in contrast to activation by TNF-α, p65 levels then declined rapidly and showed only slight peaks of activation at 2.5 h and 5.5 h. NF-κB p50 also showed a distinct initial peak at 30 min, followed by a more sustained activation during the next 8 h. NFATc2 reached maximal nuclear levels at 30 min before declining to basal levels by 2.5 h, whereas NFATc1 levels gradually increased before reaching maximal levels between 2.5 h and 8 h after TCR stimulation.

NFAT is not required for HIV transcription in Jurkat T-cells following TCR activation

Since NFATc1 is induced in response to TCR signaling, it is possible that it contributes to HIV transcription under these conditions. To test this possibility, we used cyclosporin A (CsA) to block the Ca^{2+}–calcineurin activation pathway. Control experiments demonstrated that CsA was able to completely block the induction of both NFATc1 and NFATc2 but did not prevent NF-κB p65 or p50 induction (data not shown). Flow cytometry (Fig. 1a) demonstrated that CsA did not block proviral reactivation following stimulation of either TNF-α or TCR, suggesting that not only is NFAT dispensable for proviral reactivation but sufficient levels of NF-κB p65 were induced under both conditions to drive HIV transcription.

Kinetics of HIV transcription in response to TCR signaling

In order to study early events during the induction of transcription from the latent HIV proviruses, we performed quantitative chromatin immunoprecipitation (ChIP) assays using an RNAP II antibody (Fig. 2). The ChIP assays were used to measure the accumulation of RNAP II at the TAR near the promoter (+30 to +134), which provides an accurate estimate of transcription initiation rates. In addition, RNAP II levels at a downstream region (+2593 to +2691) were measured to provide an assessment of transcription elongation efficiencies.

The data shown in Fig. 2 are a subset of an extensive data set used to simultaneously monitor HIV transcription and gene expression from control cellular genes that are responsive to NF-κB and NFAT. The ChIP data were analyzed by fitting a series of Gaussian distributions. This procedure effectively allows for the objective identification of the main peaks of transcription and the relative contribution of successive waves of transcription factor activation to overall transcription. The full data set is provided as Supplementary Data along with details of the curve fitting.

As we have previously reported, a low level of RNAP II transcription complexes accumulates near the start site of the transcription of latent HIV proviruses.[25,50,51] Both TNF-α stimulation and α-CD3/α-CD28 mAb costimulation led to the rapid recruitment of RNAP II to the HIV promoter concomitantly with the initial rise of NF-κB levels in the nucleus. Under both stimulation conditions, RNAP II accumulation at the promoter reached maximal levels at 30 min and was nearly identical during the first 90 min.

Following the initial cycle of transcription initiation, the kinetics of HIV proviral reactivation after TNF-α treatment and TCR stimulation diverged significantly. In the case of TNF-α activation, transcription initiation rebounded by 3.5 h and increased throughout the subsequent cycles of NF-κB p65 entry into the nucleus during the next 8 h. By contrast, following TCR activation, maximal HIV transcription initiation was achieved during the first cycle, and lower levels of transcription initiation were observed during each of the later time points.

The IκBα (nuclear factor of κ light polypeptide gene enhancer in B-cell inhibitor, α) gene, which is highly dependent on NF-κB for transcription initiation but does not require Tat for transcription elongation, was analyzed in parallel with the HIV provirus in order to provide an internal control for NF-κB activity (Fig. 2b). Accumulation of RNAP II near the promoter of the IκBα gene (+155 to +237) was used as a measurement of transcription initiation, while accumulation of RNAP II in a downstream region (+2038 to +2159) was used to evaluate transcription elongation. As in the case of the HIV provirus, there was a rapid increase in the transcription initiation of the IκBα gene during the first cycle of NF-κB p65 entry into the nucleus, and the first peak of transcription initiation was nearly identical following either TNF-α activation or TCR stimulation. However, comparing the patterns of IκBα gene transcription and HIV proviral transcription at later times demonstrates that the HIV promoter is more strongly stimulated and sustains a higher level of transcription than the IκBα gene between 2 h and 8 h. Similarly, following TCR activation, the IκBα gene responds poorly after the initial cycle of activation, whereas there is substantial HIV transcription under these conditions. The simplest explanation for these kinetic differences is that NF-κB p65 is the primary factor driving IκBα gene transcription throughout the time course, whereas in response to TCR signaling, additional factors help to sustain HIV transcription following the initial phase of NF-κB p65 activation.

TCR activation stimulates HIV transcriptional elongation

Although the induction of HIV transcription initiation by TNF-α was very efficient during the first cycle of NF-κB p65 entry into the nucleus, downstream RNAP II levels remained at extremely low levels at this time and only began to rise after 2 h of stimulation when the Tat protein began to accumulate.[25,33] In contrast, stimulation of 2D10 cells by α-CD3/α-CD28 antibodies strongly induced elongation during the first 90 min, a time prior to the synthesis of the new Tat protein. Integration under the fitted curves demonstrated that although initiations during the first cycle of transcription are nearly identical when cells are stimulated by TNF-α and through the TCR, elongation is approximately twice as efficient following TCR activation.

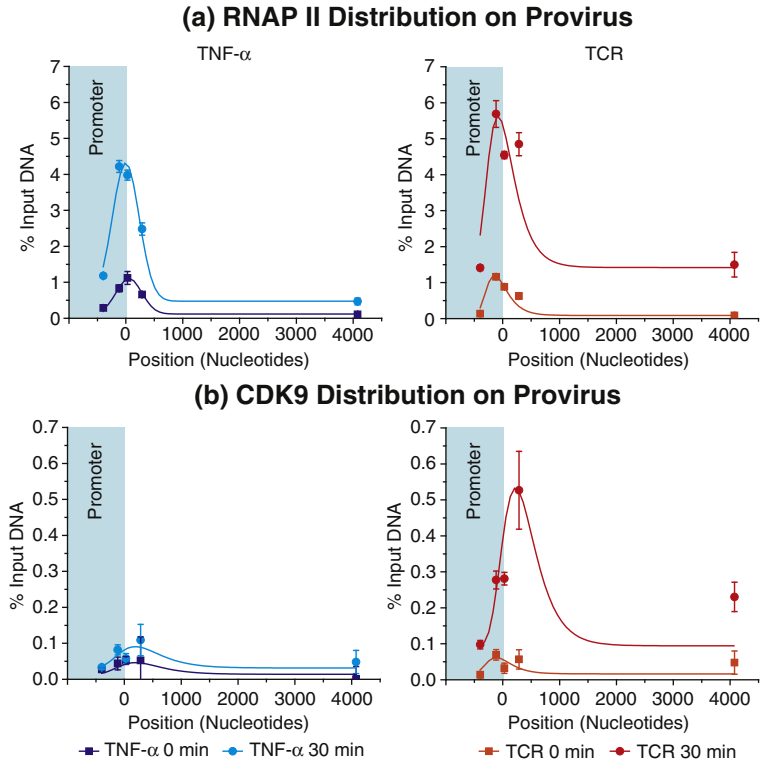

Fig. 3. Enhanced recruitment of P-TEFb to HIV proviruses following TCR activation. ChIP assays were used to measure the distribution of RNAP II and CDK9 at multiple locations along the HIV provirus. (a) RNAP II distributions. Left: 2D10 cells induced with 10 ng/ml TNF-α for 30 min (light-blue circle) and uninduced controls (dark-blue squares). Right: Cells induced for 30 min with 0.125 μg/ml α-CD3 mAb plus 1 μg/ml α-CD28 mAb (red circles) and uninduced controls (orange squares). (b) CDK9 distributions from the same experiments as shown in (a). Note that activation of cells through the TCR simultaneously stimulates P-TEFb recruitment and RNAP II elongation, but TNF-α stimulation has only minimal effects on the P-TEFb recruitment.

Changes in the elongation efficiency of the HIV provirus and the IκBα gene following activation by TNF-α or TCR stimulation were estimated by taking the ratio of RNAP II at the promoter and downstream regions for the HIV provirus (Fig. 2a) and the IκBα gene (Fig. 2b). Following stimulation by TNF-α, there is a progressive increase in elongation efficiency between 2 h and 8 h following an initial lag period of 2 h. Although initiation rates oscillate throughout this time course, the elongation ratios increase monotonically, suggesting that this is due to accumulation of Tat in the system. During TCR activation, changes in the elongation efficiency are apparent at the earliest time points, and maximal transcriptional elongation efficiencies are reached sooner than during TNF-α activation. Compared to the IκBα gene (Fig. 2b), the elongation efficiency of the latent HIV provirus is initially significantly more restricted (i.e., 10% *versus* 20–30%) but becomes dramatically more efficient (i.e., 75% *versus* 30%) once Tat is induced. In contrast to the results observed with the HIV provirus, the elongation efficiency from the IκBα gene remains constant during the activation time course since it is not activated by Tat.

TCR stimulation induces P-TEFb recruitment to the HIV provirus

In order to examine whether the strong activation of elongation that we observed at early times after TCR stimulation was associated with enhanced P-TEFb recruitment to the HIV provirus, we measured the levels of RNAP II and CDK9 at various regions of the HIV provirus by ChIP assays. Figure 3a shows that although the amounts of RNAP II near the transcription start site are similar after stimulation for 30 min by TNF-α and through the TCR, the amount of RNAP II found downstream of the TAR sequence was significantly higher in the TCR-activated samples. This enhanced RNAP II processivity was associated with a 3-fold to 6-fold increase in CDK9 levels in downstream regions of the provirus (Fig. 3b). Since, as described above, there is no significant increase in newly synthesized Tat until at least 120 min following stimulation by TNF-α, these results imply that TCR-mediated signaling uniquely increased the availability of either P-TEFb or Tat.

Enhanced HIV transcriptional elongation is mediated through an ERK-dependent signaling pathway

To define the molecular mechanisms responsible for increasing P-TEFb pool sizes, we treated 2D10 cells with a range of activators and inhibitors of pathways known to be induced by TCR-mediated signaling (Fig. 4). As shown in Fig. 4a, activation of the TCR led to a rapid increase in the amount of phosphorylated ERK-1/2 and phosphorylated AKT (serine/threonine protein kinase Akt) in both the nucleus and the cytoplasm. Treatment of cells with

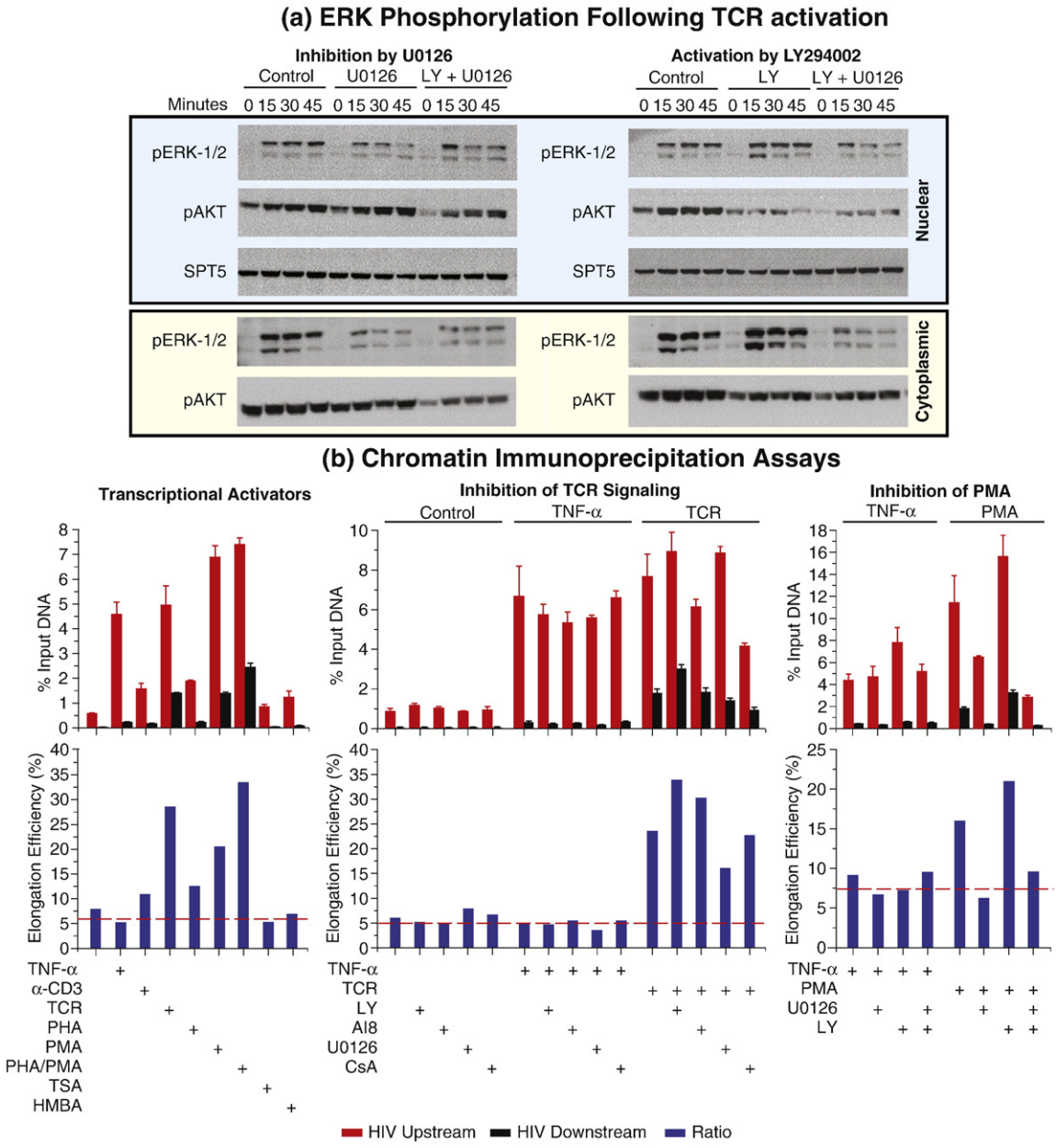

Fig. 4. ERK kinase pathway mediates TCR activation of HIV transcriptional elongation. (a) Western blot analyses. Left: Inhibition of ERK phosphorylation by U0126. 2D10 cells were induced with 0.125 μg/ml α-CD3 mAb plus 1 μg/ml α-CD28 mAb (TCR) for 30 min in the presence or in the absence of 10 μM U1026 and/or 10 μM LY294002. Nuclear and cytoplasmic extracts were blotted using antibodies against phosphorylated ERK-1/2 and phosphorylated AKT (Cell Signaling Technology). The nuclear protein Spt5 was included as loading control. Right: Activation of ERK phosphorylation by LY294002. Cells were induced through the TCR for 30 min in the presence or in the absence of 10 μM LY294002 and/or 10 μM U0126. (b) ChIP assays to measure the elongation efficiency of RNAP II on induced HIV proviruses. Left: 2D10 cells were stimulated with 5 ng/ml TNF-α (TNF); 0.125 μg/ml α-CD3 mAb (CD3); 0.125 μg/ml α-CD3 plus 1 μg/ml α-CD28 mAb, CD3 antibody (TCR); 10 μg/ml PHA (PHA); 50 ng/ml PMA (PMA); 50 ng/ml PMA plus 10 μg/ml PHA; 500 nM TSA (TSA); and 5 mM HMBA for 30 min. Center: Control 2D10 cells or cells activated with TNF-α or through the TCR for 30 min. The cells were pretreated for 1 h as follows: 10 μM LY294002 (LY); 1 μM Akt inhibitor 8 (AI8); and 10 μM U0126 (U0126) or 1 μg/ml CsA. Right: Cells activated with TNF-α or PMA for 30 min. The cells were pretreated with either 20 μM U0126 or 10 μM LY294002 for 1 h. Red bars: RNAP II levels at the transcription start site (+30 to +134. Black bars: RNAP II levels and at the downstream region (+4076 to +4172). Blue bars: Elongation efficiency as measured by the ratio of the downstream RNAP II level to the upstream RNAP II level. Broken line indicates the average elongation efficiency of unstimulated cells.

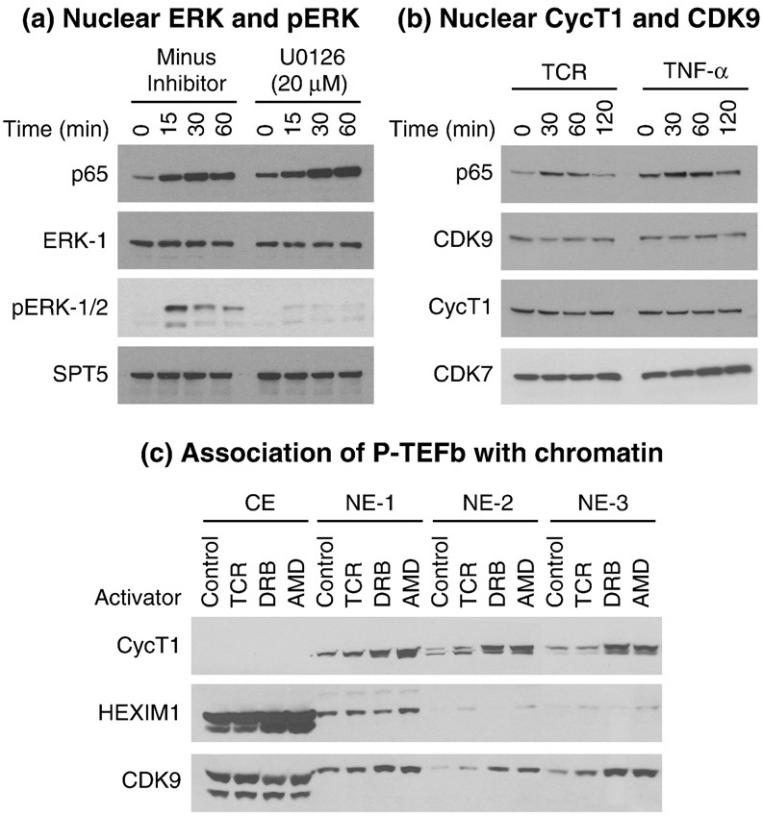

Fig. 5. P-TEFb association with chromatin is enhanced following TCR activation in the absence of new P-TEFb subunit synthesis. (a) Western blot analysis showing nuclear levels of p65, ERK-1, phosphorylated ERK-1/2 (pERK-1/2), and Spt5 following TCR activation. Left: 2D10 cells were stimulated with 0.125 μg/ml α-CD3 plus 1 μg/ml α-CD28 mAb, CD3 antibody (TCR) for up to 60 min. Right: Cells stimulated in the presence of 20 μM U0126. Note that TCR stimulation strongly increases the levels of pERK-1/2 but does not alter the total levels of nuclear ERK-1. (b) Western blot analysis showing nuclear levels of p65, CDK9, CycT1, and CDK7 following activation through the TCR (left) or by 10 ng/ml TNF-α (right). Note that the nuclear levels of CDK9 and CycT1 are unaltered compared to the CDK7 control. (c) TCR signaling enhances the association of P-TEFb with chromatin. 2D10 cells were treated with 0.125 μg/ml α-CD3 plus 1 μg/ml α-CD28 mAb, CD3 antibody (TCR); or 100 -μM DRB or 1 μg/ml actinomycin D (-AM D) for 60 min. Nuclei were prepared and extracted as described in Materials and Methods. The cytoplasmic and nuclear extracts were examined by Western blot analysis using antibodies to CycT1, HEXIM1, and CDK9.

U0126, an inhibitor of the kinase activity of mitogen-activated protein kinase kinase (MAPKK), selectively blocked ERK-1/2 phosphorylation but did not affect AKT phosphorylation. Conversely, treatment of cells with LY294002, a selective phosphatidylinositol 3-kinase (PI3K) inhibitor, blocked AKT phosphorylation and increased ERK-1/2 phosphorylation, since blocking of the AKT pathway removes an inhibitor of the ERK pathway.[52,53] For example, in the experiment shown in Fig. 4a, at 15 min after TCR stimulation, phospho-ERK-2 levels were 2.9-fold higher in cells treated with LY294002 than in control cells, and phosho-ERK-1 levels were 1.7-fold higher than in control cells. Treating cells with a combination of LY294002 and U0126 reduced ERK-2 levels to 60% of the control values.

ChIP assays were performed to study the effects of these inhibitors and a range of transcription activation conditions on transcription elongation. In the experiments shown in Fig. 4b, RNAP II levels were measured both at an upstream site (+30 to +134) and at a downstream site (+2593 to +2691), and the ratio was used to estimate the elongation efficiency, as described above. Exposure of 2D10 cells to TNF-α, phytohemagglutinin (PHA), trichostatin A (TSA), or hexamethylene bisacetamide (HMBA) did not cause any significant changes in elongation efficiency at 30 min following treatment. However, activation by phorbol 12-myristate 13-acetate (PMA) and by a combination of PMA and PHA strongly induced elongation at 30 min poststimulation.

In cells activated either through the TCR or by PMA, exposure to U0126 reduced the elongation efficiency by approximately 50% but had no significant effect on initiation (Fig. 4b). By contrast, the AKT inhibitors LY294002 and AI8 (Akt inhibitor 8) were able to further activate transcriptional elongation following TCR stimulation or PMA activation. Since U0126 is able to partially reverse the effects of LY294002, it seems likely that the enhancement in elongation that we have observed is due to the enhanced activation of ERK-1/2 mediated by AKT inhibition.

Control experiments confirmed that none of the inhibitors studied affected transcriptional elongation in untreated cells or in cells activated by TNF-α (Fig. 4b). Finally, we note that blocking of NFAT activation by CsA had no impact on transcription elongation (Fig. 4b).

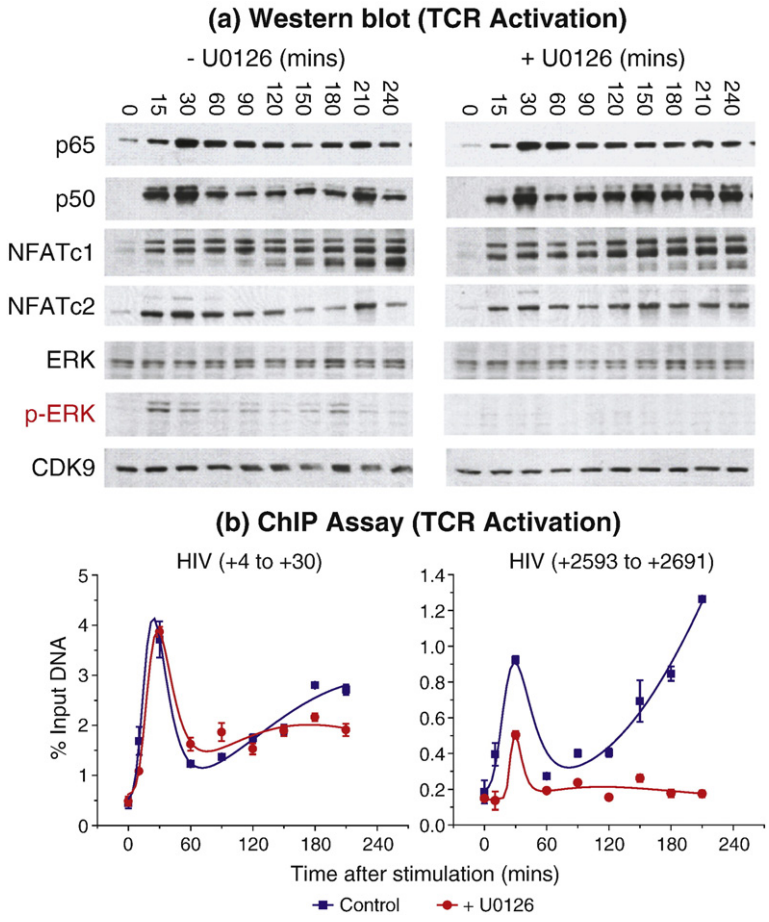

Fig. 6. U0126 blocks TCR-mediated HIV transcription elongation. (a) Western blot analysis showing an accumulation of the transcription factors NF-κB and NFAT in the nucleus after the activation of cells with 0.125 μg/ml α-CD3 mAb plus 1 μg/ml α-CD28 mAb, either in the absence of U0126 or after pretreatment with 10 μM U0126, for 1 h. Included in the blot are analyses of the nuclear levels of ERK-1/2 and phospho-ERK. (b) The distribution of RNAP II on the HIV provirus measured by ChIP assays following TCR activation. U0126 had little effects on RNAP levels upstream (+30 to +134), but it significantly reduced the amount of RNAP downstream (+2593 to 2691).

CycT1 and CDK9 levels are not altered in response to TCR signaling

The signaling events stimulated by the TCR could either result in an enhanced synthesis of the components of the transcription elongation machinery, such as CycT1 and CDK9, or act to enhance their activity by inducing posttranscriptional modifications. To distinguish between these two possibilities, we undertook additional Western blot analysis experiments to test whether nuclear ERK, CycT1, and CDK9 levels were altered within the first 2 h after TCR activation. As shown in Fig. 5a, nuclear ERK-1 levels remain constant during the first hour after TCR activation. By contrast, high levels of phosphorylated ERK-1/2 appear in the nucleus within 15 min and then slowly decay. Consistent with the results shown in Fig. 4a, the phosphorylation of ERK-1/2 is blocked by U0126.

There are no detectable changes in the nuclear levels of CycT1, CDK9, or CDK7 during the first 2 h after TCR stimulation (Fig. 5b). The constitutive expression of CycT1 and CDK9 in Jurkat T-cells is in contrast to the situation in primary resting memory T-cells and monocytes, where CycT1 is low prior to TCR stimulation and new CycT1 is synthesized within 60 min.[24,48,49]

TCR signaling induces global increases in P-TEFb association with chromatin

In order to test whether TCR signaling induced a general increase in transcription associated with P-TEFb recruitment to the chromatin, we performed Western blot analyses on a series of nuclear extracts (Fig. 5c). In Jurkat T-cells, there is an excess of HEXIM1 and CDK9, which can be detected at high levels in cytoplasmic extracts prepared in hypotonic buffers. CycT1 is absent from these fractions. By contrast, nuclear extracts prepared using buffers containing 0.36 M NaCl contain stoichiometric amounts of CycT1 and CDK9 and variable amounts of HEXIM1. The initial nuclear extracts contain high levels of HEXIM1, suggesting that they are enriched in the nucleoplasmic 7SK RNP complex. Subsequent extracts, which represent fractions that are more tightly associated with the chromatin, contain only CycT1 and CDK9. Treatment of cells with either DRB or actinomycin D, which induces dissociation of the 7SK RNP complex[37,38] (see also Fig. 8), induced an increased association of the CycT1 and CDK9 subunits of P-TEFb with chromatin but did not alter HEXIM1 levels in the nuclear extracts. Similarly, TCR signaling induced a global increase

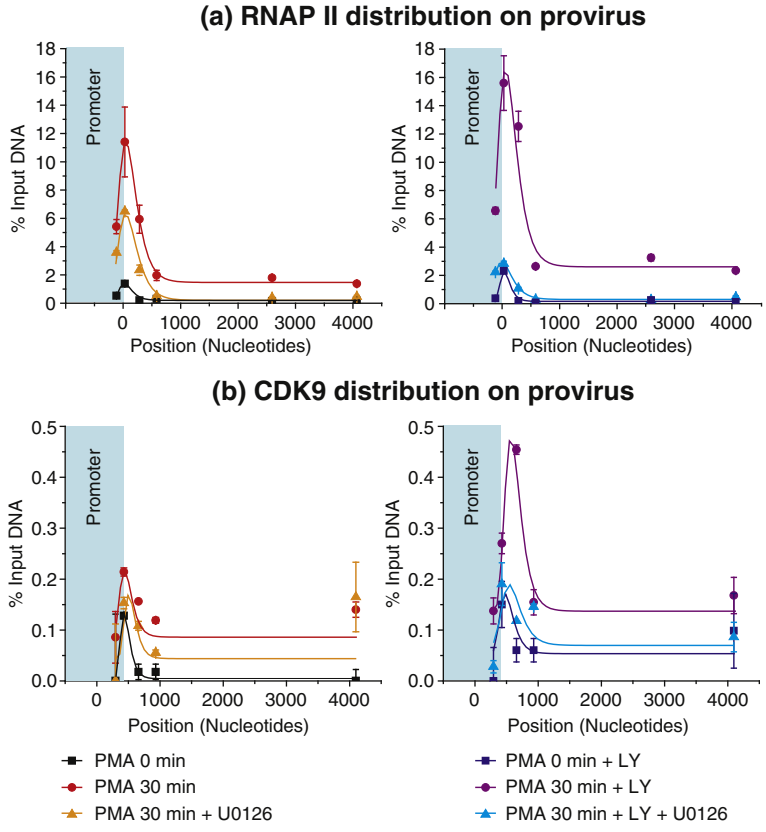

Fig. 7. Recruitment of P-TEFb to HIV proviruses following PMA activation is blocked by U0126 and enhanced by LY294002. ChIP assays were used to measure the distribution of RNAP II and CDK9 at multiple locations along the HIV provirus genome. (a) RNAP II distributions. Left: Cells induced with 50 ng/ml PMA for 30 min (red circles), cells induced with PMA in the presence of 20 μM U0126 (yellow triangles), and uninduced controls (black squares). Right: Cells induced with 50 ng/ml PMA and 10 μM LY294002 for 30 min (purple circles), cells induced with PMA and LY294002 in the presence of 20 μM U0126 (light-blue triangles), and uninduced controls (dark-blue squares). (b) CDK9 distributions from the same experiments as shown in (a).

in P-TEFb association with the chromatin. This is consistent with the ChIP data presented in Fig. 3, demonstrating that TCR signaling increased the levels of CDK9 recruited to latent HIV proviruses.

Thus, the activation of elongation on HIV by the TCR signaling that we have observed seems to be associated with an ERK-mediated posttranslation modification of presynthesized P-TEFb rather as the result of the new synthesis of its subunits.

U0126 blocks TCR activation of HIV transcriptional elongation

To verify that elongation is selectively activated early after TCR activation, we performed time-course experiments similar to those shown in Fig. 2 in the presence and in the absence of U0126. U0126 selectively blocked ERK phosphorylation, but it did not interfere with NF-κB p65 and p50 translocation to the nucleus following TCR (Fig. 6a). U0126 also had no impact on NFATc1 and NFATc2 activation. In the corresponding ChIP experiments, U0126 treatment did not inhibit RNAP II recruitment to the promoter but did result in a dramatic decrease in HIV elongation during the first wave of transcription (Fig. 6b). Similarly, U0126 is able to restrict transcriptional elongation and CDK9 recruitment following PMA stimulation of cells (data not shown). U0126 also strongly inhibits HIV elongation during the 2-h to 4-h period when Tat synthesis has resumed. Complementary studies using PD98059, which inhibits the dephosphorylated form of MAPKK1 and blocks the induction of AP-1 (activator protein 1) during TCR signaling, have shown that it contributes to HIV transcription during the 2-h to 4-h period but plays no role during the first round of HIV elongation between 0 h and 2 h (J.H., U.M., & J.K., unpublished results).

Recruitment of P-TEFb to HIV proviruses following PMA activation is blocked by U0126 and enhanced by LY294002

The inhibitor studies shown in Fig. 4 strongly suggested that both TCR activation and PMA stimulation enhanced HIV transcription elongation through a common mechanism involving the ERK kinase pathway. To confirm that PMA stimulation of cells resulted in enhanced P-TEFb recruitment to the HIV provirus, we performed additional ChIP experiments (Fig. 7).

Activation of cells for 30 min with PMA stimulated RNAP II recruitment to the provirus, transcriptional elongation, and CDK9 recruitment. Recruitment of both RNAP II and CDK9 was strongly inhibited by treatment with U0126. Importantly, treatment of cells with a combination of PMA and LY294002 boosted the levels of both

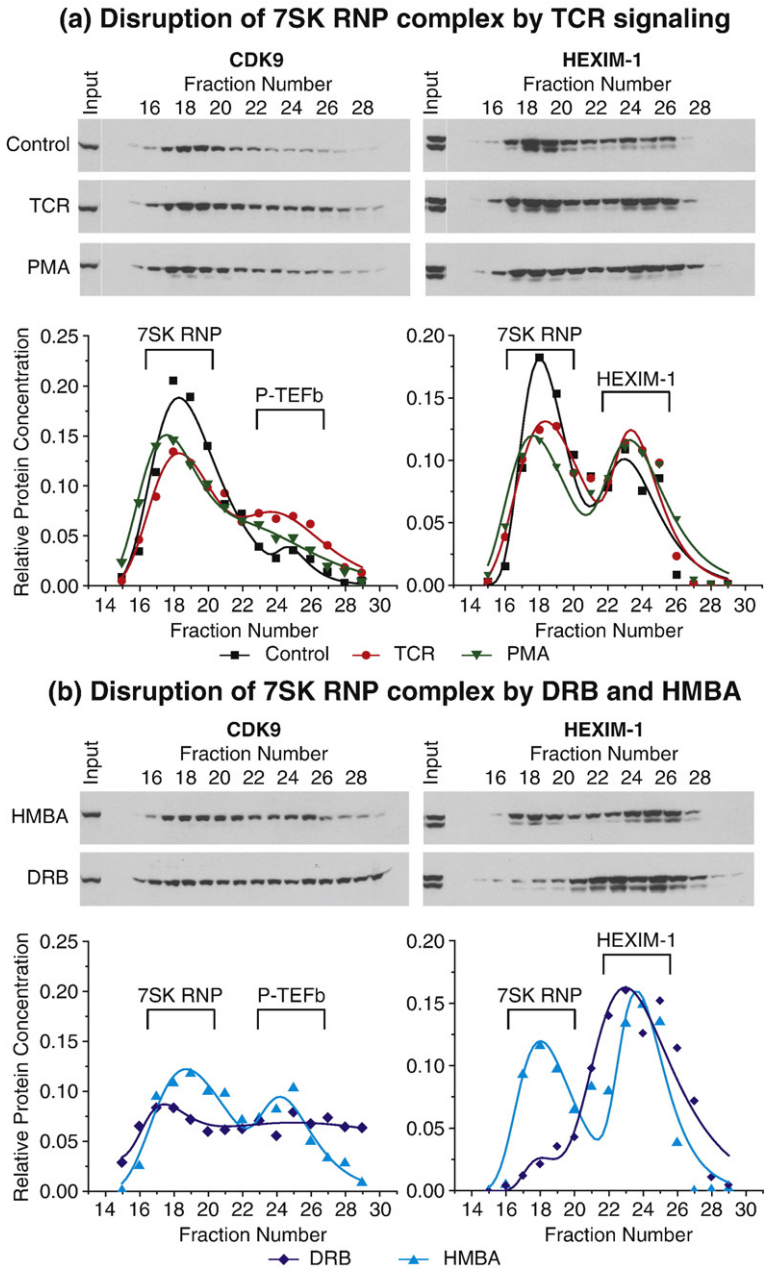

Fig. 8. TCR signaling induces the disassembly of the 7SK RNP complex. Whole-cell lysates were fractionated on Superdex 200 gel-filtration columns. Quantitative Western blot analysis was performed to examine the chromatography profiles of CDK9 (left) and HEXIM1 (right). Top: Western blot analyses. Bottom: Elution profiles based on a densitometry analysis of Western blot analyses. (a) Disruption of 7SK complexes by TCR signaling. Jurkat 2D10 cells were treated with 0.125 μg/ml α-CD3 mAb plus 1 μg/ml α-CD28 mAb for 30 min. (b) Disruption with 10 mM HMBA, or with 100 μM DRB for 1 h.

RNAP II and CDK9 associated with the activated HIV provirus and was inhibited by U0126. Thus, the amounts of RNAP II and CDK9 associated with the HIV provirus varied in proportion to the degree of ERK activation.

Disruption of the 7SK RNP complex is mediated by ERK

The preceding data strongly suggest that restrictions imposed on P-TEFb activity in resting T-cells can be relieved through activation of the MAPKK/ERK pathway. We therefore decided to investigate whether TCR activation could alter the levels of the 7SK RNP complex found in T-cells.

As shown in Fig. 8a, fractionation of Jurkat T-cell extracts by gel-filtration chromatography demonstrates that the majority of P-TEFb is found as part of the large 7SK RNP complex. Integration of the areas under the peaks showed that in the unstimulated cells, 95% of CDK9 and 68% of HEXIM1 in the cell are associated with the large complex, while 5% of CDK9 and 32% of HEXIM1 are associated with the low-molecular-weight fraction. Thus, there is a

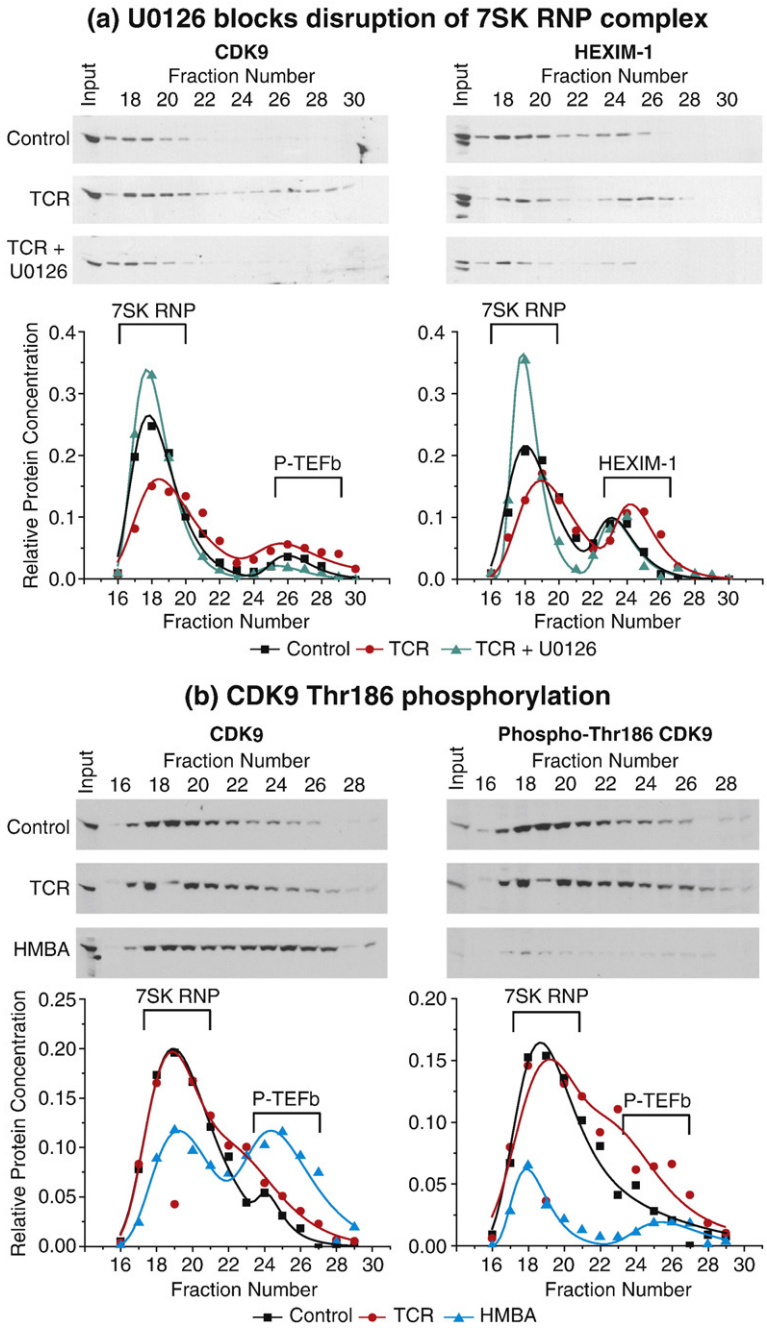

Fig. 9. The ERK pathway mediates the disassembly of the 7SK RNP complex in response to TCR activation. Whole-cell lysates were fractionated on Superdex 200 gel-filtration columns. Quantitative Western blot analysis was performed to examine the chromatography profiles of CDK9 (left) and HEXIM1 (right). Top: Western blot analyses. Bottom: Elution profiles based on a densitometry analysis of Western blot analyses. (a) U0126 blocks the disruption of the 7SK complex induced by TCR activation. Jurkat 2D10 cells were treated for 30 min with 0.125 μg/ml α-CD3 mAb plus 1 μg/ml α-CD28 mAb, with or without 1 h of pretreatment with 10 μM U0126. The panel shows Western blot analysis and chromatography profiles of CDK9 (left) and HEXIM1 (right). (b) CDK9 present in P-TEFb released by TCR activation remains phosphorylated on the T-loop. Jurkat 2D10 cells were treated with either α-CD3/α-CD28 antibodies or 5 mM HMBA for 30 min. The panel shows Western blot analysis and chromatography profiles of CDK9 (left) and phospho-Thr186 CDK9 (right).

significantly higher proportion of CDK9 associated with the 7SK RNP complex in Jurkat T-cells than has been observed in the more extensively studied HeLa cells, where typically less than 50% of P-TEFb in the cell is in the large complex.[37,38,46,54]

As shown in Fig. 8a, stimulation of the cells for 30 min through the TCR or by exposure to PMA results in a significant disruption of the large complex and in the release of P-TEFb into a low-molecular-weight fraction. Following TCR treatment, 29% of CDK9 and 35% of HEXIM1 are found in the lower-molecular-weight fractions. The degree of complex dissociation following TCR signaling is comparable to the disruption seen following a 30-min exposure to HMBA (low-molecular-weight fraction: CDK9, 26%; HEXIM1, 47%), but less than that induced by DRB (low-molecular-weight fraction: CDK9, 60%; HEXIM1, 88%) (Fig. 8b).

U0126 effectively blocks the disruption of the 7SK RNP complex by TCR signaling. In the experiment shown in Fig. 9a, 12% of CDK9 and

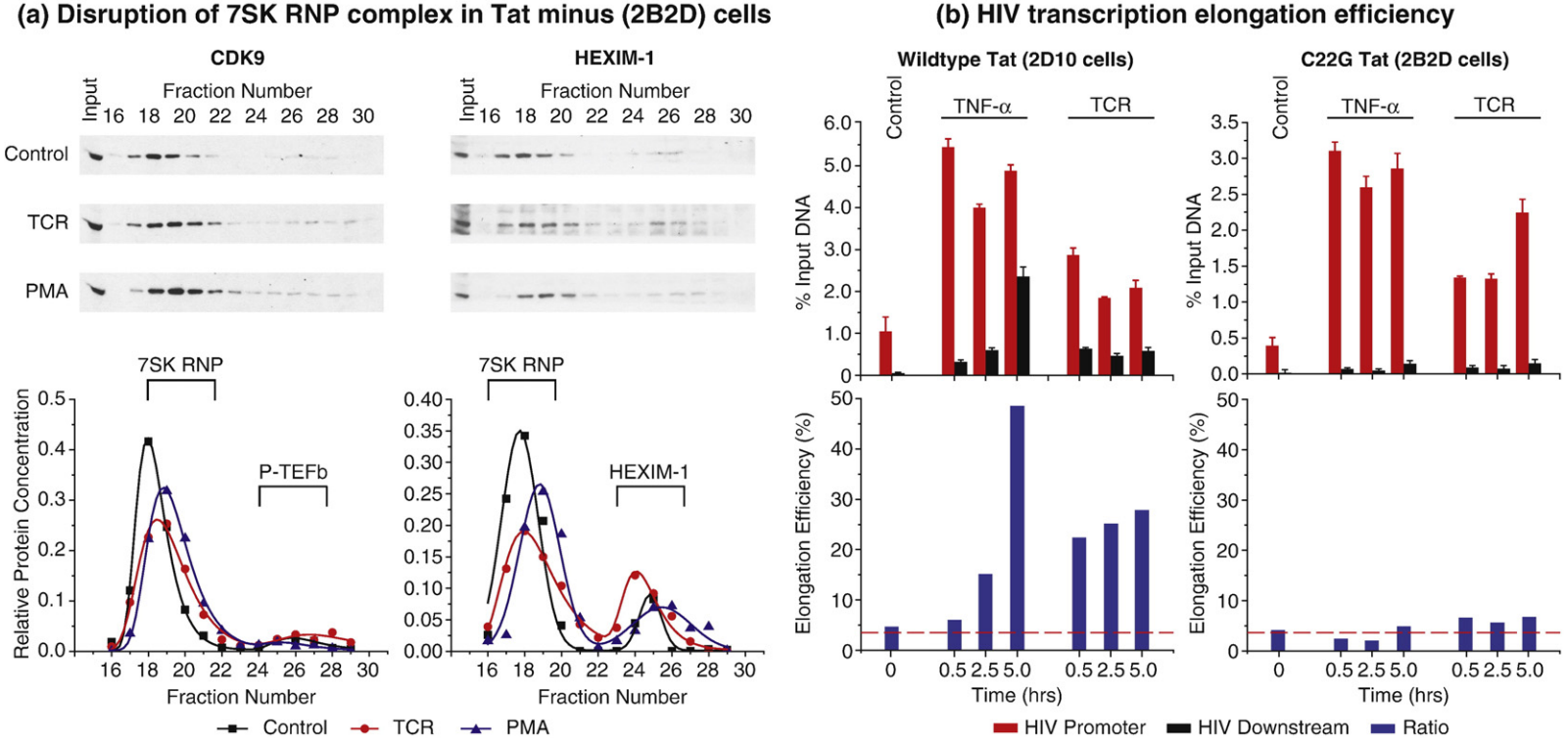

Fig. 10. Disruption of the 7SK RNP complex in response to TCR activation occurs in the absence of HIV Tat. (a) Disruption of the 7SK RNP complex in Tat$^-$ (2B2D) cells. Whole-cell lysates were fractionated on Superdex 200 gel-filtration columns, and quantitative Western blot analysis was performed to examine the chromatography profiles of CDK9 (left) and HEXIM1 (right). Top: Western blot analyses. Bottom: Elution profiles based on a densitometry analysis of Western blot analyses. (b) HIV transcription elongation efficiency. ChIP assays were performed as described in the legend to Fig. 4b. Left: 2D10 cells were stimulated for 0.5 h, 2.5 h, or 10 h with either 5 ng/ml TNF-α (TNF) or 0.125 μg/ml α-CD3 plus 1 μg/ml α-CD28 mAb, CD3 antibody (TCR). Right: 2B2D cells were stimulated for 0.5 h, 2.5 h, or 10 h with either 5 ng/ml TNF-α (TNF) or 0.125 μg/ml α-CD3 plus 1 μg/ml α-CD28 mAb, CD3 antibody (TCR). Top, red bars: RNAP II levels at the transcription start site (+30 to +134). Top, black bars: Downstream region (+4076 to +4172). Bottom, blue bars: Elongation efficiency as measured by the ratio of the downstream RNAP II levels to the upstream RNAP II level. Broken line indicates the average elongation efficiency of unstimulated or TNF-α-stimulated cells.

26% of HEXIM1 were found initially in the low-molecular-weight fraction. After stimulation of the TCR for 30 min, 22% of CDK9 and 31% of HEXIM1 were found in the low-molecular-weight fraction. Treatment with U0126 not only blocked TCR-induced dissociation but resulted in a slightly greater accumulation of CDK9 and HEXIM1 in the 7SK RNA/P-TEFb/HEXIM1 complex than in unstimulated cells (93% CDK9 and 88% HEXIM1 in the complex). This strongly suggests that the ERK signaling is responsible for the release of the functional P-TEFb that we have described above.

Although activation of cells through the TCR or by PMA and treatment with HMBA and DRB all resulted in 7SK RNP disruption, only activation by TCR or PMA resulted in enhanced HIV elongation efficiencies. Since DRB is also an inhibitor of CDK9 activity, it would be expected to only release inactive P-TEFb.

The failure of HMBA to stimulate HIV transcription elongation appears to be associated with the phosphorylation state of CDK9. Enzymatically active CDK9 must be phosphorylated on Thr186. As shown in Fig. 9b, disruption of the 7SK RNP complex by TCR signaling resulted in the release of CDK9 that remains phosphorylated on Thr186. In this experiment, 95% of the CDK9 in the unstimulated cells remained associated with the large complex, and 5% was found in the small complex. Similarly, the large complex contained 92% of the phospho-Thr-CDK9 in the extract, while the small complex contained 8%. After TCR stimulation, 21% of the total CDK9 and 11% of phospho-Thr-CDK9 were released into the small complex. However, as originally reported by Chen *et al.*, although HMBA induced the release of 45% of the CDK9 into the small complex, the released P-TEFb was extensively dephosphorylated on Thr186.[54] For example, the amount of phospho-Thr-CDK9 in the small complex following HMBA treatment corresponded to only 18% of the total CDK9.

TCR-mediated disruption of the 7SK RNP complex does not require Tat

Previous studies have documented that Tat acts to disrupt the 7SK RNP complex by competing with HEXIM for CycT1 binding.[44–46] In order to determine whether the residual Tat present in the latently infected 2D10 cells could be contributing to the disruption of the 7SK RNAP complex, we measured the dissociation of the 7SK RNP complex in response to TCR signaling and PMA treatment in 2B2D cells,[25] which harbor a latent provirus carrying the inactive C22G mutation in Tat, preventing its interactions with P-TEFb (Fig. 10). As shown in Fig. 10a, both TCR and PMA are able to induce 7SK RNP complex disruption in 2B2D cells at levels comparable to those seen in 2D10 cells. For example, in the uninduced cells, 86.5% of HEXIM1 is found in the 7SK RNP complex, and 13.5% is found in the low-molecular-weight fraction. After induction through the TCR or by PMA treatment, the amount of HEXIM1 in the low-molecular-weight fraction more than doubles (29.8% TCR and 27.0% PMA).

Subthreshold levels of Tat contribute to HIV reactivation in latently infected cells

To evaluate whether P-TEFb released by TCR signaling in 2B2D cells required Tat in order to activate HIV transcription elongation, we used ChIP assays to compare the HIV transcription elongation efficiencies in 2D10 and 2B2D cells at 0.5 h, 2.5 h, and 5 h after activation (Fig. 10b). Consistent with the results described above, stimulation of both cells for 0.5 h with TNF-α did not increase the elongation efficiency above the basal level of 4.2 ± 1.5% in either cell line. However, activation of the TCR for 0.5 h increased the HIV elongation efficiency to 22.3% in TCR-stimulated 2D10 cells, but only to 6.5% in 2B2D cells.

Consistent with the results shown Fig. 2, there was a dramatic increase in HIV elongation efficiency at 2.5 h (15.0%) and 5.0 h (48.4%) after activation by TNF-α due to the resumption of Tat synthesis from the reactivated provirus. There was only a modest further increase in elongation efficiency at 2.5 h (25.0%) and 5.0 h (27.7%) after TCR stimulation compared to the already high levels of elongation observed at 0.5 h (22.3%). By contrast, in 2B2D cells, the elongation efficiency remains only slightly elevated, with an average value of 6.2 ± 0.6% for the time points 0.5 h, 2.5 h, and 5.0 h.

Thus, the increase in HIV elongation efficiency that we have observed following TCR stimulation appears to require a combination of P-TEFb activation and Tat availability. As described above, since there is no new synthesis of P-TEFb subunits following TCR activation, these data suggest that there is either activation of residual Tat activity in 2D10 cells or new synthesis of Tat that does not occur after TNF-α stimulation (see Discussion).

In conclusion, our data demonstrate that functional P-TEFb can be released through an ERK-dependent cell signaling pathway. This previously uncharacterized signaling pathway represents one of the first examples of the physiological enhancement of P-TEFb activity and transcriptional elongation.

Discussion

Kinetics of HIV proviral reactivation

The strong conservation of a large number of cis-acting DNA elements in the HIV-1 LTR implies that a

concerted action of numerous regulatory elements is needed to ensure a robust production of viral mRNA in activated cells.[55] In this article, we have begun to dissect how TCR-mediated signaling pathways contribute to the reactivation of latent HIV proviruses using the extensively characterized 2D10 cells as a model system.[25,51] A significant advantage of the 2D10 clone is that it is also readily inducible by a wide range of activators although it is highly restricted in unstimulated cells (Fig. 1). Importantly, 2D10 cells, which are derived from the Jurkat T-cell clone E6 selected to carry a functional TCR signaling apparatus, are also highly responsive to activation by treatment with mAbs directed against the CD3 receptor and the CD28 coactivator. As shown here, stimulation of the TCR activates an ordered program of transcription factor entry into the nucleus with early mobilization of NF-κB and NFATc1, succeeded by mobilization of NFATc2.

Our experiments take advantage of the high degree of synchrony observed in T-cells following TCR activation, which permits us to measure the oscillations in transcription activity that are associated with the rapid exchange of transcription factors between the nucleus and the cytoplasm. A second critical element in our studies is the use of quantitative ChIP assays to detect the distribution of RNAP II at various sites along the integrated HIV proviral genome. By comparing the concentration of RNAP II near the transcription start site to that in downstream sites, we have been able to obtain accurate measurements of transcription initiation rates and elongation efficiencies. Because the ChIP assay directly measures RNAP II densities during transcription, it provides a much more accurate measurement of rapid changes in transcription than more traditional measurements based on the accumulation of a transcribed or translated product. Using these techniques, we have been able to observe how periodic fluctuations in HIV transcription initiation on the order of 60–90 min (Fig. 3) overlap with the progressive long-term changes in HIV transcription elongation efficiencies that occur due to the accumulation of Tat over an 8-h time course (Fig. 6).

A key conclusion arising from these analyses is that the first wave of HIV transcription initiation following TCR activation is driven primarily, if not exclusively, by NF-κB. Although TCR activation also induces NFATc1 and NFATc2, which are fully functional and can support the transcription of NFAT-responsive genes such as EGR2 and TNF-α (Supplementary Data), it is dispensable for HIV transcription since there is no significant change in RNAP II recruitment to the provirus when NFAT activation is blocked by treatment with CsA (Fig. 1). Furthermore, there were no measurable changes in HIV transcription initiation and elongation during the first 4 h after TCR induction when cells are treated with cyclosporine (data not shown). This suggests that NF-κB induced by TCR signaling effectively competes with NFAT for HIV LTR binding.[56,57]

Regulation of P-TEFb by ERK kinases enhances HIV transcriptional elongation

Although the first round of HIV transcription initiation induced by the stimulation of both TNF-α and TCR is mediated by NF-κB, and RNAP II recruitment to the provirus shows nearly identical kinetics and levels under both conditions, dramatic differences in transcription elongation are evident even at the earliest times. As shown by multiple experiments, there is always an enhanced level of transcription elongation when cells are stimulated through the TCR compared to transcription elongation observed when cells are stimulated by TNF-α. This correlates with a dramatic increase in P-TEFb (CDK9) recruitment to the provirus, especially in downstream regions where elongation complexes accumulate (Fig. 3). It is important to note that the enhanced P-TEFb recruitment can be easily observed at 30 min, which is a time during the first phase of transcription prior to the accumulation of newly synthesized Tat (see the text below).

Experiments using a variety of transcriptional activators and small-molecule inhibitors of cell signaling pathways demonstrate that P-TEFb activation is mediated by ERK kinases (Figs. 4–6). First, U0126, which is a potent inhibitor of ERK kinase activation, inhibits transcriptional elongation and P-TEFb recruitment to the HIV provirus in cells that have been activated either through the TCR or by PMA. Second, enhanced transcriptional elongation and P-TEFb recruitment can also be observed following activation of cells by PMA, a phorbol ester that activates protein kinase C and results in NF-κB mobilization, as well as activation of the ERK kinase pathway. Finally, treatment of cells with LY294002, which inhibits the AKT pathway, results in enhanced ERK phosphorylation following cell stimulation[52,53,58] and a corresponding increase in transcription elongation and P-TEFb recruitment to HIV proviruses (Figs. 4 and 6). Thus, we can correlate the extent of transcriptional elongation with the extent of ERK phosphorylation. Inhibitors that block ERK phosphorylation (such as U0126) also block HIV transcription, whereas compounds that enhance ERK phosphorylation (such as LY294002) stimulate HIV transcription elongation and P-TEFb recruitment.

Direct evidence that P-TEFb is activated following TCR activation comes from experiments measuring the release of P-TEFb from the large 7SK RNP complex (Figs. 7–9). Extensive disruption of the large complex is observed within 30 min of TCR stimulation. As expected, TCR-mediated 7SK RNP

complex disruption can be blocked by treatment of cells with U0126 (Fig. 9).

Our results are consistent with two earlier reports suggesting that either the ERK pathway or TCR signaling could activate P-TEFb. Fujita *et al.* observed that thyrotropin-releasing hormone can induce the recruitment of P-TEFb and transcription elongation to immediate early genes (c-*fos*, JunB, and mitogen-activated protein kinase-1) in neuroendocrine GH4C1 cells.[59] Importantly, as in our study, the ERK signaling pathway is activated by thyrotropin-releasing hormone in these cells, and transcription elongation could be blocked by U0126. Second, while this work was in progress, Natarajan *et al.* reported that TCR signaling can enhance HIV transcription by stimulating the dissociation of both NF-κB and P-TEFb.[58] While their conclusions are similar to ours, the two studies differ because Natarajan *et al.* did not demonstrate directly that there was dissociation of the large 7SK RNP complex, nor did they show a direct effect of TCR signaling on HIV transcription elongation.[58]

Regulation of P-TEFb by HMBA is distinct from activation of P-TEFb via the TCR

Previous studies have shown that disruption of P-TEFb complexes by HMBA can result in enhanced HIV transcriptional activity; however, there have been conflicting claims about the mechanism of action of HMBA. Contreras *et al.* reported that HMBA can activate the PI3K/AKT pathway, which leads to the phosphorylation of HEXIM1 and the subsequent release of active pools of P-TEFb.[60] However, this mechanism does not appear to be responsible for the enhanced HIV transcription elongation that we have observed, since inhibitors of the PI3K/AKT pathway, such as AKT8 and LY294002, not only do not block HIV transcription but actually enhance it. An alternative mechanism for the HMBA activation of HIV transcription was suggested by Choudhary *et al.*, who reported that HMBA signaling is mediated via both protein kinase Cμ and PI3K.[61] Our observation that LY294002 stimulates HIV elongation also rules out this mechanism as being responsible for the TCR-mediated activation of P-TEFb.

A third activation mechanism for the activation of HIV transcription by HMBA—that HMBA-induced release of P-TEFb from 7SK small nuclear RNP is mediated by the calcium ion (Ca^{2+})–calmodulin–protein phosphatase 2B signaling pathway—has been reported by Chen *et al.*[54] In the mechanism that they described, Ca^{2+} signaling alone is insufficient to activate P-TEFb, and (Ca^{2+})–calmodulin–protein phosphatase 2B acts sequentially and cooperatively with protein phosphatase-1α, which releases P-TEFb by dephosphorylating phospho-Thr186 in the CDK9 T-loop. Our data are most consistent with these findings. We have found that treatment of cells with HMBA for 30 min effectively disrupts the large 7SK RNP complex (Fig. 8) but does not stimulate transcriptional elongation under these conditions (Fig. 4), presumably because dephosphorylation of the T-loop of CDK9 inactivates the enzyme (Fig. 9). Since HMBA can reactivate HIV proviruses over longer periods of time, it is reasonable to assume that, at some later stage, the dephosphorylated enzyme released from the 7SK RNP complex can become rephosphorylated.

Tat-dependent and Tat-independent transcriptional elongation during HIV proviral reactivation

As shown in Fig. 1, the HIV promoter is initially more restricted for transcriptional elongation than the promoter of the NF-κB-responsive gene IκBα. As we will describe elsewhere, this additional restriction on elongation is due primarily to the enhanced recruitment of NELF to RNAP II initiating on latent proviruses due to the affinity of the NELF-E subunit for TAR RNA. As transcription proceeds, the new Tat protein begins to accumulate after a lag of approximately 2 h, and HIV transcriptional elongation efficiency becomes boosted to levels that are eventually over 3-fold higher than the levels observed in the NF-κB-dependent cellular genes IκBα and JunB.

During TCR signaling, dissociation of the large 7SK RNP complex increases the pool of active P-TEFb in the cell and enhances HIV transcriptional elongation. This results in both a global increase in the association of P-TEFb with chromatin (Fig. 5) and increased HIV transcription. Activation of P-TEFb in response to TCR signaling does not require Tat, since dissociation of the 7SK RNP complex can be observed in 2B2D cells[25] that harbor a latent provirus carrying the C22G mutation in Tat, which prevents its interactions with P-TEFb (Fig. 10).

Tat levels in the latently infected 2D10 cells are extremely low and are below the level of detection by Western blot analysis (data not shown). Further evidence that there are only minimal Tat levels in latently infected cells comes from the observation that there is no HIV transcription in these cells above the basal activity seen in Tat^{-} cells (Fig. 10). Nonetheless, activation of P-TEFb via the TCR results in a disproportionate increase in HIV elongation at early time points in cells latently infected with proviruses that carry a functional Tat gene.

Where does this "new" P-TEFb/Tat activity come from? Our preferred hypothesis is that the latently infected 2D10 cells carry subthreshold levels of presynthesized Tat. We suggest that posttranslational modification of the components of the 7SK RNP complex through the TCR signaling pathway leads to the rapid disruption of the complex and increases the pool of active P-TEFb in the cell. The newly released P-TEFb is then able to associate with the residual Tat and to enhance HIV transcriptional

elongation. This hypothesis is based on the assumption that 15–30 min is an insufficient period of time to induce new HIV transcription and to synthesize new Tat. For example, we have observed that following TNF-α activation of HIV transcription, there is a lag period of approximately 2 h prior to the enhancement of HIV transcription elongation, which correlates closely with the kinetics of new Tat synthesis from latent proviruses reported by Williams *et al.*[33] An alternative hypothesis is that TCR signaling is able to induce new Tat synthesis in the absence of new mRNA synthesis. For example, it is possible that there is a residual pool of Tat mRNA that is restricted by miRNA or some other translational control mechanism that is regulated through the TCR. Although we are unable to formally rule out this hypothesis at this stage, we note that both Tat protein levels and Tat mRNA levels remain at extremely low levels during the first 2 h following TCR activation of 2D10 cells and do not increase measurably (data not shown).

It remains an open question whether P-TEFb can ever be recruited to the HIV LTR in the absence of Tat. Recent studies of lipopolysaccharide-inducible primary response genes in macrophages have suggested that P-TEFb can be recruited to cellular promoters via Brd4, which both binds P-TEFb and can recognize chromatin-carrying H4K5/8/12Ac markers.[62] However, this mechanism does not apply to latent HIV proviruses, which characteristically show dramatically reduced acetylated histone levels compared to cellular primary response genes such as IκBα.[25] The inability to efficiently recruit P-TEFb to HIV proviruses in the absence of Tat may be an important mechanism contributing to the maintenance of proviral latency.

Mobilization of P-TEFb in primary resting central memory T-cells

Stimulation of the TCR by foreign antigens is believed to be the major physiological mechanism used to reactivate latent HIV proviruses. In addition to engagement of the TCR itself, several costimulatory molecules, including CD28, stimulate a series of signaling cascades leading to T-cell proliferation, cytokine production, and differentiation into effector cells. We have recently shown using a model for HIV latency in primary resting memory T-cells that TNF-α treatment efficiently activates NF-κB but fails to activate P-TEFb. By contrast, TCR signaling induces both NF-κB and P-TEFb[24] and is therefore able to activate latent HIV proviruses.

In contrast to Jurkat T-cells, primary resting central memory T-cells show highly restricted levels of CycT1 and the presence of CDK9 that is inactive because of the dephosphorylation of the critical Thr186 in the T-loop.[47] Activation of P-TEFb in these cells therefore requires multiple steps involving both the initial assembly of the 7SK RNP complex and its relocalization to nuclear speckles, where it becomes accessible to the transcription machinery. It remains to be determined how the ERK-dependent signaling pathway we have identified in Jurkat T-cells contributes to the regulation of P-TEFb in the primary T-cells; however, it is of interest to note that PMA can enhance CDK9 T-loop phosphorylation more than 10-fold in primary resting T-cells.[47]

Therapeutic implications

Currently, extensive efforts are being exerted to devise "shock-and-kill" strategies for HIV eradication.[8,63,64] In these strategies, a "shock" phase is used to reactivate latent proviruses, while a "kill" phase is used to eliminate cells induced through immune responses, viral cytopathogenicity, or cytotoxic drugs. In devising these strategies, emphasis has been placed on using either histone deacetylase inhibitors (such as SAHA, suberoylanilide hydroxamic acid)[65,66] or activators of NF-κB[67,68] to reactivate the latent proviruses. Our observations that P-TEFb activation enhances the reactivation of latent proviruses suggests that effective activation of the entire latent viral pool may ultimately require cocktails of drugs that stimulate both transcription initiation and P-TEFb mobilization.

Materials and Methods

Materials

RPMI 1640 medium and fetal bovine serum were purchased from Hyclone. HMBA, DRB, PHA, and LY294002 were obtained from Sigma. U0126 was purchased from Calbiochem. α-CD3 and α-CD28 antibodies were obtained from BD Biosciences. HEXIM1 antibody was custom-synthesized by Covance Research Products. Phosphor-ERK 1/2 (Thr202/Tyr204), phospho-AKT (Thr308), and phospho-CDK9 (Thr186) antibodies were obtained from Cell Signaling Technology. All other antibodies used in this study were purchased from Santa Cruz Biotechnology.

Cell culture and reactivation of clones

Isolation and reactivation of the 2D10 and 2B2D clones had been described previously by Pearson *et al.*[25] The 2D10 clone contains attenuated H13L Tat, and 2B2D has C22G mutation in Tat that is devoid of transactivation activity. Cells were maintained with RPMI 1640 medium supplemented with 10% fetal bovine serum, penicillin (100 IU/ml), streptomycin (100 μg/ml), and 25 mM Hepes at 37 °C in 5% CO_2. The cells were reactivated with 10 ng/ml TNF-α; 0.125 μg/ml α-CD3 mAb plus 1 μg/ml α-CD28 mAb; 0.125 μg/ml α-CD3 antibody; 10 μg/ml PHA;

50 ng/ml PMA; 50 ng/ml PMA plus 10 μg/ml PHA; and 500 nM TSA or 5 mM HMBA, as indicated, for 18 h and analyzed for d2EGFP expression by fluorescence-activated cell sorting.

Nuclear protein analysis

Nuclear protein was obtained as described by Hoffmann *et al.*[69] Briefly, 5×10^6 cells were collected and washed with ice-cold phosphate-buffered saline. The cells were resuspended in cytosolic extract lysis buffer (10 mM Hepes–KOH, 60 mM KCl, 1 mM ethylenediaminetetraacetic acid, 0.5% NP-40, 1 mM DTT, and 1 mM PMSF) containing a cocktail of protease inhibitors (Roche) and incubated on ice for 10 min. Cells were vortexed, and nuclei were pelleted by centrifugation for 10 min at 4000 rpm. Nuclei were resuspended in 60 μl of NE buffer [250 mM Tris (pH 7.8), 60 mM KCl, 1 mM ethylenediaminetetraacetic acid, 1 mM DTT, and 1 mM PMSF] containing protease inhibitors, and the nuclear proteins were extracted by several freeze–thaw cycles. Protein concentrations were determined using the BCA protein assay kit (Pierce) or the Bradford reagent (Bio-Rad). The NuPAGE system (Invitrogen) was used to resolve proteins on a 10% 2-[bis(2-hydroxyethyl)amino]-2-(hydroxymethyl)propane-1,3-diol (Bistris) gel. Western blot analysis was performed with antibodies against NF-κB p65, NF-κB p50, NFATc1, NFATc2, Spt5, phospho-ERK 1/2 (Thr202/Tyr204), phospho-AKT (Thr308), and CDK9.

ChIP assay

2D10 cells were incubated with TNF-α (10 μg/ml) or 0.125 μg/ml α-CD3 mAb plus 1 μg/ml α-CD28 mAb (TCR) for 0–8 h. When indicated, 2D10 cells were preincubated for 1 h in the presence of inhibitors. Fifty million cells were isolated from the population for each time point in the reactivation time course. Each sample was immediately fixed with 0.5% of formaldehyde and prepared for ChIP, as previously described.[50] The antibodies used for immunoprecipitation were total RNAP II (N-20; Santa Cruz Biotechnology) and CDK9 (H-169; Santa Cruz Biotechnology). Real-time PCR was preformed by using 2% of each precipitated DNA. Percentage input for each data was determined by comparing the C_t value of each sample to a C_t standard curve generated from a serial dilution of genomic DNA. A no-antibody control value was subtracted from each sample value to remove the nonspecific background signal. The primers used are as follows: HIV (promoter) −116 F-AGC TTG CTA CAA GGG ACT TTC C, HIV +4 R-ACC CAG TAC AGG CAA AAA GCA G; HIV (Nuc-1 position) +30 F-CTG GGA GCT CTC TGG CTA ACT A, HIV +134 R-TTA CCA GAG TCA CAC AAC AGA CG; HIV +283 F-GAC TGG TGA GTA CGC CAA AAA T, HIV +390 R-TTT CCC ATC GCG ATC TAA TTC; HIV +584 F-AGC AAC CCT CTA TTG T GT GCA T, +683 R-TGC GGT GGT CTT ACT TTT GTT T; HIV (env position) +2593 F-TGA GGG ACA ATT GGA GAA GTG A, HIV +2691 R-TCT GCA CCA CTC TTC TCT TTG C; HIV (d2EGFP position) +4076 F-GAC AAG CAG AAG AAC GGC ATC, HIV +4172 R-GGG TGT TCT GCT GGT AGT GGT; IκBα +155 F-AAG AAG GAG CGG CTA CTG GAC, IκBα +237 R-TCC TTG ACC ATC TGC TCG TAC T; IκBα +2038 F-ATG CAG CCA TAA GCA TCT CAA A, IκBα +2159 R-CCC ACA CTT CAA CAG GAG TGA C; IκBα 2871 F-TGG TAG GAT CAG CCC TCA TTT T, IκBα 2978 R-AAC CCC ACA AAG GTG AGG TTT A.

Analysis of P-TEFb complexes in Jurkat cell lysates

Jurkat 2D10 or 2B2D cells were either untreated or treated for 30 min with either 0.125 μg/ml α-CD3 mAb plus 1 μg/ml α-CD28 mAb, 50 ng/ml PMA, or 10 mM HMBA, or for 1 h with 100 μM DRB. A total of 5×10^7 cells were lysed, and nuclear proteins were extracted in cell lysis buffer A [10 mM Hepes (pH 8.0), 150 mM NaCl, 10 mM KCl, 1.5 mM $MgCl_2$, 0.5% NP-40, 1 mM DTT, and 1 mM PMSF] containing a protease inhibitor cocktail and, where indicated, phosphatase inhibitors. Whole-cell lysates were centrifuged at 5000 rpm for 10 min, and the supernatant was loaded onto a Superdex 200 resin in a Tricorn 10/300 sizing column. One bed volume of cell lysis buffer A was used for elution, and 500-μl fractions were collected. Methanol–chloroform precipitation was used to concentrate proteins in the collected fractions. The protein pellets corresponding to fractions 15–29 were resuspended under reducing conditions in 1× SDS sample buffer, heated at 95 °C for 10 min, then loaded onto a 10% Bistris denaturing gel. Quantitative Western blot analyses of the eluates were performed to examine the chromatography profiles of CDK9, phospho-Thr186 CDK9, and HEXIM1.

P-TEFb association with chromatin

A total of 1×10^7 2D10 cells were stimulated by 10 ng/ml TNF-α or 0.125 μg/ml α-CD3 plus 1 μg/ml α-CD28 mAb, collected, and washed with ice-cold phosphate-buffered saline. The cells were resuspended in hypotonic buffer [10 mM KCl, 4 mM $MgCl_2$, 10 mM Hepes (pH 7.9), 2 mM DTT, 750 mM spermidine, 150 mM spermine, and protease inhibitor cocktail] and then homogenized. Nuclei were pelleted, and the supernatant was collected as cytosolic extract. The nuclei were incubated in a 1:1 solution of high-salt buffer (0.72 M KCl) and hypotonic buffer with periodic vortexing for 30 min at 4 °C and then pelleted by centrifugation to obtain the first extract (NE-1). The nuclear pellet was incubated as described above with NE buffer containing 360 mM KCl to obtain the second extract (NE-2). The residual pellet was placed in 0.1% SDS buffer and sonicated. The solubilized fraction from the residual pellet was designated as NE-3. Protein concentrations were determined using the BCA protein assay kit (Pierce). The NuPAGE system (Invitrogen) was used to resolve 15 mg of total nuclear proteins on a 4–12% Bistris gel. Western blot analysis was performed with antibodies against CycT1, HEXIM1, and CDK9.

Data analysis

Flow cytometry data were analyzed using FloJo. Gates for viable cells in the population (typically over 90% for unstimulated cells and over 80% for stimulated cells) were set based on forward light scatter and side light scatter. Gates for d2EGFP were determined using uninfected Jurkat cells as negative control and stimulated 2D10 cells as positive control.

Origin Pro (version 7.5) was used to generate curve fits for each of the data sets shown in Figs. 2, 3, 6–10, and 9. The ChIP time-course data sets shown in Figs. 2 and 6 were fitted to a series of overlapping skewed Gaussian distributions (see equation below). The baseline y_0 was fixed to perform the fits, and 100 sequential iterations were used to find optimal parameters for the peak center xc_n, the amplitude A, and the peak width w for each peak. The derivative of the original data set was used to objectively identify the number and approximate position of the peaks. To further refine the fits, we fixed xc values for individual peaks in succession, and we iteratively calculated values for the amplitude and peak width until minimal χ^2 values had been obtained.

The column chromatography data (Figs. 8–10) were fitted, using an analogous procedure, to a series of overlapping skewed Gaussian functions of the form:

$$y = y_0 + Ae^{(-e^{-z}-z+1)};\ z = (x - xc) / w$$

The data in Fig. 2 showing the calculated elongation efficiencies were fitted either to the Boltzmann distribution or to straight lines. The data in Fig. 7, showing the distribution of RNAP II and P-TEFb along the proviral genome, were fitted to a single skewed Gaussian.

Acknowledgements

We thank past and present members of the Karn laboratory: Richard Pearson, Julian Wong, Julia Friedman, Mudit Tyagi, Kara Lassen, Hongxia Mao, Michael Greenberg, Amy Graham, Won Kyung Cho, and Julie Jadlowsky for their help and useful discussions. This work was supported by grants R01-AI067093 and DP1-DA028869 from the National Institutes of Health to J.K. Additional support came from grant 106639-38-RFRL from amfAR (The Foundation for AIDS Research) to Y.K.K. J.H. was supported by the AIDS International Training and Research Program (5D43-TW00011) from Fogarty International Center at the National Institutes of Health. We also thank the Case Western Reserve University/University Hospitals Center for AIDS Research (P30-AI036219) for provision of flow cytometry services.

Supplementary Data

Supplementary data to this article can be found online at doi:10.1016/j.jmb.2011.03.054

References

1. Pierson, T., McArthur, J. & Siliciano, R. F. (2000). Reservoirs for HIV-1: mechanisms for viral persistence in the presence of antiviral immune responses and antiretroviral therapy. *Annu. Rev. Immunol.* **18**, 665–708.
2. Coiras, M., Lopez-Huertas, M. R., Perez-Olmeda, M. & Alcami, J. (2009). Understanding HIV-1 latency provides clues for the eradication of long-term reservoirs. *Nat. Rev. Microbiol.* **7**, 798–812.
3. Alexaki, A., Liu, Y. & Wigdahl, B. (2008). Cellular reservoirs of HIV-1 and their role in viral persistence. *Curr. HIV Res.* **6**, 388–400.
4. Chun, T. W., Davey, R. T., Jr., Engel, D., Lane, H. C. & Fauci, A. S. (1999). Re-emergence of HIV after stopping therapy. *Nature*, **401**, 874–875.
5. Davey, R. T., Jr., Bhat, N., Yoder, C., Chun, T. W., Metcalf, J. A., Dewar, R. *et al.* (1999). HIV-1 and T cell dynamics after interruption of highly active antiretroviral therapy (HAART) in patients with a history of sustained viral suppression. *Proc. Natl Acad. Sci. USA*, **96**, 15109–15114.
6. Fischer, M., Hafner, R., Schneider, C., Trkola, A., Joos, B., Joller, H. *et al.* (2003). HIV RNA in plasma rebounds within days during structured treatment interruptions. *AIDS*, **17**, 195–199.
7. Dinoso, J. B., Kim, S. Y., Wiegand, A. M., Palmer, S. E., Gange, S. J., Cranmer, L. *et al.* (2009). Treatment intensification does not reduce residual HIV-1 viremia in patients on highly active antiretroviral therapy. *Proc. Natl Acad. Sci. USA*, **106**, 9403–9408.
8. Richman, D. D., Margolis, D. M., Delaney, M., Greene, W. C., Hazuda, D. & Pomerantz, R. J. (2009). The challenge of finding a cure for HIV infection. *Science*, **323**, 1304–1307.
9. Shen, L. & Siliciano, R. F. (2008). Viral reservoirs, residual viremia, and the potential of highly active antiretroviral therapy to eradicate HIV infection. *J. Allergy Clin. Immunol*, **122**, 22–28.
10. Trono, D., Van Lint, C., Rouzioux, C., Verdin, E., Barre-Sinoussi, F., Chun, T. W. & Chomont, N. (2010). HIV persistence and the prospect of long-term drug-free remissions for HIV-infected individuals. *Science*, **329**, 174–180.
11. Peterlin, B. M. & Price, D. H. (2006). Controlling the elongation phase of transcription with P-TEFb. *Mol. Cell*, **23**, 297–305.
12. Karn, J. (2011). The molecular biology of HIV latency: breaking and restoring the Tat-dependent transcriptional circuit. *Curr. Opin. HIV AIDS*, **6**, 4–11.
13. Singh, A. & Weinberger, L. S. (2009). Stochastic gene expression as a molecular switch for viral latency. *Curr. Opin. Microbiol.* **12**, 460–466.
14. Wei, P., Garber, M. E., Fang, S. M., Fischer, W. H. & Jones, K. A. (1998). A novel cdk9-associated c-type cyclin interacts directly with HIV-1 Tat and mediates its high-affinity, loop specific binding to TAR RNA. *Cell*, **92**, 451–462.
15. Fujinaga, K., Irwin, D., Huang, Y., Taube, R., Kurosu, T. & Peterlin, B. M. (2004). Dynamics of human immunodeficiency virus transcription: P-TEFb phosphorylates RD and dissociates negative effectors from the transactivation response element. *Mol. Cell. Biol.* **24**, 787–795.
16. Kim, Y. K., Bourgeois, C. F., Isel, C., Churcher, M. J. & Karn, J. (2002). Phosphorylation of the RNA polymerase II carboxyl-terminal domain by CDK9 is directly responsible for human immunodeficiency virus type 1 Tat-activated transcriptional elongation. *Mol. Cell. Biol.* **22**, 4622–4637.
17. Bourgeois, C. F., Kim, Y. K., Churcher, M. J., West, M. J. & Karn, J. (2002). Spt5 cooperates with Tat by

preventing premature RNA release at terminator sequences. *Mol. Cell. Biol.* **22**, 1079–1093.
18. Ivanov, D., Kwak, Y. T., Guo, J. & Gaynor, R. B. (2000). Domains in the SPT5 protein that modulate its transcriptional regulatory properties. *Mol. Cell. Biol.* **20**, 2970–2983.
19. Weinberger, L. S., Burnett, J. C., Toettcher, J. E., Arkin, A. P. & Schaffer, D. V. (2005). Stochastic gene expression in a lentiviral positive-feedback loop: HIV-1 Tat fluctuations drive phenotypic diversity. *Cell*, **122**, 169–182.
20. Weinberger, L. S., Dar, R. D. & Simpson, M. L. (2008). Transient-mediated fate determination in a transcriptional circuit of HIV. *Nat. Genet.* **40**, 466–470.
21. Keedy, K. S., Archin, N. M., Gates, A. T., Espeseth, A., Hazuda, D. J. & Margolis, D. M. (2009). A limited group of class I histone deacetylases act to repress human immunodeficiency virus type-1 expression. *J. Virol.* **83**, 4749–4756.
22. Williams, S. A., Chen, L. F., Kwon, H., Ruiz-Jarabo, C. M., Verdin, E. & Greene, W. C. (2006). NF-kappaB p50 promotes HIV latency through HDAC recruitment and repression of transcriptional initiation. *EMBO J.* **25**, 139–149.
23. Tyagi, M. & Karn, J. (2007). CBF-1 promotes transcriptional silencing during the establishment of HIV-1 latency. *EMBO J.* **26**, 4985–4995.
24. Tyagi, M., Pearson, R. J. & Karn, J. (2010). Establishment of HIV latency in primary $CD4^+$ cells is due to epigenetic transcriptional silencing and P-TEFb restriction. *J. Virol.* **84**, 6425–6437.
25. Pearson, R., Kim, Y. K., Hokello, J., Lassen, K., Friedman, J., Tyagi, M. & Karn, J. (2008). Epigenetic silencing of human immunodeficiency virus (HIV) transcription by formation of restrictive chromatin structures at the viral long terminal repeat drives the progressive entry of HIV into latency. *J. Virol.* **82**, 12291–12303.
26. du Chene, I., Basyuk, E., Lin, Y. L., Triboulet, R., Knezevich, A., Chable-Bessia, C. *et al.* (2007). Suv39H1 and HP1gamma are responsible for chromatin-mediated HIV-1 transcriptional silencing and post-integration latency. *EMBO J.* **26**, 424–435.
27. Marban, C., Suzanne, S., Dequiedt, F., de Walque, S., Redel, L., Van Lint, C. *et al.* (2007). Recruitment of chromatin-modifying enzymes by CTIP2 promotes HIV-1 transcriptional silencing. *EMBO J.* **26**, 412–423.
28. Blazkova, J., Trejbalova, K., Gondois-Rey, F., Halfon, P., Philibert, P., Guiguen, A. *et al.* (2009). CpG methylation controls reactivation of HIV from latency. *PLoS Pathog.* **5**, e1000554.
29. Kauder, S. E., Bosque, A., Lindqvist, A., Planelles, V. & Verdin, E. (2009). Epigenetic regulation of HIV-1 latency by cytosine methylation. *PLoS Pathog.* **5**, e1000495.
30. Han, Y., Lin, Y. B., An, W., Xu, J., Yang, H. C., O'Connell, K. *et al.* (2008). Orientation-dependent regulation of integrated HIV-1 expression by host gene transcriptional readthrough. *Cell Host Microbe*, **4**, 134–146.
31. Lenasi, T., Contreras, X. & Peterlin, B. M. (2008). Transcriptional interference antagonizes proviral gene expression to promote HIV latency. *Cell Host Microbe*, **4**, 123–133.
32. Duverger, A., Jones, J., May, J., Bibollet-Ruche, F., Wagner, F. A., Cron, R. Q. & Kutsch, O. (2009). Determinants of the establishment of human immunodeficiency virus type 1 latency. *J. Virol.* **83**, 3078–3093.
33. Williams, S. A., Kwon, H., Chen, L. F. & Greene, W. C. (2007). Sustained induction of NF-kappaB is required for efficient expression of latent human immunodeficiency virus type 1. *J. Virol.* **81**, 6043–6056.
34. Bosque, A. & Planelles, V. (2008). Induction of HIV-1 latency and reactivation in primary memory $CD4^+$ T cells. *Blood*, **113**, 58–65.
35. Nabel, G. & Baltimore, D. A. (1987). An inducible transcription factor activates expression of human immunodeficiency virus in T cells. *Nature*, **326**, 711–713.
36. Kinoshita, S., Su, L., Amano, M., Timmerman, L. A., Kaneshima, H. & Nolan, G. P. (1997). The T cell activation factor NF-ATc positively regulates HIV-1 replication and gene expression in T cells. *Immunity*, **6**, 235–244.
37. Nguyen, V. T., Kiss, T., Michels, A. A. & Bensaude, O. (2001). 7SK small nuclear RNA binds to and inhibits the activity of CDK9/cyclin T complexes. *Nature*, **414**, 322–325.
38. Yang, Z., Zhu, Q., Luo, K. & Zhou, Q. (2001). The 7SK small nuclear RNA inhibits the CDK9/cyclin T1 kinase to control transcription. *Nature*, **414**, 317–322.
39. Yik, J. H., Chen, R., Nishimura, R., Jennings, J. L., Link, A. J. & Zhou, Q. (2003). Inhibition of P-TEFb (CDK9/Cyclin T) kinase and RNA polymerase II transcription by the coordinated actions of HEXIM1 and 7SK snRNA. *Mol. Cell*, **12**, 971–982.
40. Michels, A. A., Fraldi, A., Li, Q., Adamson, T. E., Bonnet, F., Nguyen, V. T. *et al.* (2004). Binding of the 7SK snRNA turns the HEXIM1 protein into a P-TEFb (CDK9/cyclin T) inhibitor. *EMBO J.* **23**, 2608–2619.
41. He, N., Jahchan, N. S., Hong, E., Li, Q., Bayfield, M. A., Maraia, R. J. *et al.* (2008). A La-related protein modulates 7SK snRNP integrity to suppress P-TEFb-dependent transcriptional elongation and tumorigenesis. *Mol. Cell*, **29**, 588–599.
42. Krueger, B. J., Jeronimo, C., Roy, B. B., Bouchard, A., Barrandon, C., Byers, S. A. *et al.* (2008). LARP7 is a stable component of the 7SK snRNP while P-TEFb, HEXIM1 and hnRNP A1 are reversibly associated. *Nucleic Acids Res.* **36**, 2219–2229.
43. Jeronimo, C., Forget, D., Bouchard, A., Li, Q., Chua, G., Poitras, C. *et al.* (2007). Systematic analysis of the protein interaction network for the human transcription machinery reveals the identity of the 7SK capping enzyme. *Mol. Cell*, **27**, 262–274.
44. Barboric, M., Yik, J. H., Czudnochowski, N., Yang, Z., Chen, R., Contreras, X. *et al.* (2007). Tat competes with HEXIM1 to increase the active pool of P-TEFb for HIV-1 transcription. *Nucleic Acids Res.* **35**, 2003–2012.
45. Sedore, S. C., Byers, S. A., Biglione, S., Price, J. P., Maury, W. J. & Price, D. H. (2007). Manipulation of P-TEFb control machinery by HIV: recruitment of P-TEFb from the large form by Tat and binding of HEXIM1 to TAR. *Nucleic Acids Res.* **35**, 4347–4358.
46. Krueger, B. J., Varzavand, K., Cooper, J. J. & Price, D. H. (2010). The mechanism of release of P-TEFb and HEXIM1 from the 7SK snRNP by viral and

cellular activators includes a conformational change in 7SK. *PLoS One*, **5**, e12335.
47. Ramakrishnan, R., Dow, E. C. & Rice, A. P. (2009). Characterization of Cdk9 T-loop phosphorylation in resting and activated CD4(+) T lymphocytes. *J. Leukocyte Biol.* **86**, 1345–1350.
48. Dow, E. C., Liu, H. & Rice, A. P. (2010). T-loop phosphorylated Cdk9 localizes to nuclear speckle domains which may serve as sites of active P-TEFb function and exchange between the Brd4 and 7SK/HEXIM1 regulatory complexes. *J. Cell. Physiol.* **224**, 84–93.
49. Sung, T. L. & Rice, A. P. (2009). miR-198 inhibits HIV-1 gene expression and replication in monocytes and its mechanism of action appears to involve repression of cyclin T1. *PLoS Pathog.* **5**, e1000263.
50. Kim, Y. K., Bourgeois, C. F., Pearson, R., Tyagi, M., West, M. J., Wong, J. *et al.* (2006). Recruitment of TFIIH to the HIV LTR is a rate-limiting step in the emergence of HIV from latency. *EMBO J.* **25**, 3596–3604.
51. Meredith, L. W., Sivakumaran, H., Major, L., Suhrbier, A. & Harrich, D. (2009). Potent inhibition of HIV-1 replication by a Tat mutant. *PLoS One*, **4**, e7769.
52. Guan, K. L., Figueroa, C., Brtva, T. R., Zhu, T., Taylor, J., Barber, T. D. & Vojtek, A. B. (2000). Negative regulation of the serine/threonine kinase B-Raf by Akt. *J. Biol. Chem.* **275**, 27354–27359.
53. Zimmermann, S. & Moelling, K. (1999). Phosphorylation and regulation of Raf by Akt (protein kinase B). *Science*, **286**, 1741–1744.
54. Chen, R., Liu, M., Li, H., Xue, Y., Ramey, W. N., He, N. *et al.* (2008). PP2B and PP1alpha cooperatively disrupt 7SK snRNP to release P-TEFb for transcription in response to Ca^{2+} signaling. *Genes Dev.* **22**, 1356–1368.
55. Pereira, L. A., Bentley, K., Peeters, A., Churchill, M. J. & Deacon, N. J. (2000). A compilation of cellular transcription factor interactions with the HIV-1 LTR promoter. *Nucleic Acids Res.* **28**, 663–668.
56. Chen-Park, F. E., Huang, D. B., Noro, B., Thanos, D. & Ghosh, G. (2002). The κB DNA sequence from the HIV long terminal repeat functions as an allosteric regulator of HIV transcription. *J. Biol. Chem.* **277**, 24701–24708.
57. Giffin, M. J., Stroud, J. C., Bates, D. L., von Koenig, K. D., Hardin, J. & Chen, L. (2003). Structure of NFAT1 bound as a dimer to the HIV-1 LTR κB element. *Nat. Struct. Biol.* **10**, 800–806.
58. Natarajan, M., August, A. & Henderson, A. J. (2010). Combinatorial signals from CD28 differentially regulate human immunodeficiency virus transcription in T cells. *J. Biol. Chem.* **285**, 17338–17347.
59. Fujita, T., Ryser, S., Piuz, I. & Schlegel, W. (2008). Up-regulation of P-TEFb by the MEK1–ERK signaling pathway contributes to stimulated transcription elongation of immediate early genes in neuroendocrine cells. *Mol. Cell. Biol.* **28**, 1630–1643.
60. Contreras, X., Barboric, M., Lenasi, T. & Peterlin, B. M. (2007). HMBA releases P-TEFb from HEXIM1 and 7SK snRNA via PI3K/Akt and activates HIV transcription. *PLoS Pathog.* **3**, 1459–1469.
61. Choudhary, S. K., Archin, N. M. & Margolis, D. M. (2008). Hexamethylbisacetamide and disruption of human immunodeficiency virus type 1 latency in CD4 (+) T cells. *J. Infect. Dis.* **197**, 1162–1170.
62. Hargreaves, D. C., Horng, T. & Medzhitov, R. (2009). Control of inducible gene expression by signal-dependent transcriptional elongation. *Cell*, **138**, 129–145.
63. Savarino, A., Mai, A., Norelli, S., El Daker, S., Valente, S., Rotili, D. *et al.* (2009). "Shock and kill" effects of class I-selective histone deacetylase inhibitors in combination with the glutathione synthesis inhibitor buthionine sulfoximine in cell line models for HIV-1 quiescence. *Retrovirology*, **6**, 52.
64. Bowman, M. C., Archin, N. M. & Margolis, D. M. (2009). Pharmaceutical approaches to eradication of persistent HIV infection. *Expert Rev. Mol. Med.* **11**, e6.
65. Archin, N. M., Espeseth, A., Parker, D., Cheema, M., Hazuda, D. & Margolis, D. M. (2009). Expression of latent HIV induced by the potent HDAC inhibitor suberoylanilide hydroxamic acid. *AIDS Res. Hum. Retroviruses*, **25**, 207–212.
66. Contreras, X., Schweneker, M., Chen, C. S., McCune, J. M., Deeks, S. G., Martin, J. & Peterlin, B. M. (2009). Suberoylanilide hydroxamic acid reactivates HIV from latently infected cells. *J. Biol. Chem.* **284**, 6782–6789.
67. Williams, S. A., Chen, L. F., Kwon, H., Fenard, D., Bisgrove, D., Verdin, E. & Greene, W. C. (2004). Prostratin antagonizes HIV latency by activating NF-kappaB. *J. Biol. Chem.* **279**, 42008–42017.
68. Yang, H. C., Xing, S., Shan, L., O'Connell, K., Dinoso, J., Shen, A. *et al.* (2009). Small-molecule screening using a human primary cell model of HIV latency identifies compounds that reverse latency without cellular activation. *J. Clin. Invest.* **119**, 3473–3486.
69. Hoffmann, A., Levchenko, A., Scott, M. L. & Baltimore, D. (2002). The IκB–NF-κB signaling module: temporal control and selective gene activation. *Science*, **298**, 1241–1245.